RADIATIVE CAPTURE OF PROTONS BY C^{12} AND C^{13}

Thesis by

John Dorrington Seagrave

In Partial Fulfillment of the Requirements

For the Degree of

Doctor of Philosophy

California Institute of Technology

Pasadena, California

1951

ACKNOWLEDGMENTS

This work was sponsored by the far-sighted joint program of the Office of Naval Research and the Atomic Energy Commission for the support of basic scientific research. I am also indebted to the ONR contract and the California Institute of Technology for research and teaching assistantships and tuition grants during the past two years.

I wish to thank Professors C. C. Lauritsen and William A. Fowler for the opportunity of working with them at the Kellogg Radiation Laboratory, and for suggesting and encouraging this investigation. I gratefully acknowledge discussion of the results with Professors R. F. Christy and T. Lauritsen, and with R. G. Thomas, R. B. Day, and J. E. Perry, Jr. I am moreover indebted to Drs. Day and Perry for the initial attack on this problem, and permission to use their results, and to Dr. Perry for his further correspondence and enthusiastic interest.

Dr. Perry was in charge of the construction of the 3 Mev Van de Graaff accelerator used in this work, and was assisted by R. B. Day, D. B. Duncan, A. B. Brown, Jr., and myself. Others of the laboratory staff who gave material assistance in design, construction, and maintenance of the equipment used in this research were V. F. Ehrgott, W. D. Gibbs, L. J. Gililland, George Fastle, and J. Hill. The author was assisted in the operation and maintenance of the accelerator by R. B. Day, Ken Reynolds, R. E. Odening, and Torben Huus, and acknowledges the collaboration of E. J. Woodbury in scintillation measurements of the N^{14} radiation.

The preparation of this thesis was facilitated by the careful and patient work of Miss Jeanne Antz in preparing the illustrations, and of Miss Mary Toyoda in typing the manuscript.

ABSTRACT

A method has been developed for preparing thin films of carbon on tantalum, and the thick and thin target yields of the (p,γ) reactions for C^{12} and C^{13} targets studied for proton energies of 0.4 to 2.7 Mev.

With C^{13} enriched targets, five resonances were found, corresponding to levels in N^{14} at 8.05, 8.62, 8.70, 9.18, and 9.49 Mev. The radiation spectrum from these levels has been investigated and found to involve several branches of decay, and transitions cascading through intermediate levels.

TABLE OF CONTENTS

I. INTRODUCTION

Nuclear reactions initiated by particle bombardment are usually considered to take place in several steps. The incident particle is first captured by the target nucleus, forming a compound nucleus, which is excited to a degree given by the expression

$$E_{ex} = (M_o + M_1 - M)\, c^2 + \frac{M_o}{M_o + M_1} E_1, \tag{1}$$

where M_o, M_1, and M are the masses of the target, incident, and compound nuclei, respectively, and E_1 is the kinetic energy of the incident particle (in the laboratory frame of reference). The factor $M_o/(M_o + M_1)$ gives the fraction of E_1 available for excitation in the center-of-mass system.

The compound nucleus persists in this state for a time long compared with its time of formation ($\backsim 10^{-21}$ seconds) but very much shorter than is directly measurable ($\ll 10^{-10}_{\text{sec.}}$). In this (relatively) long time, the nucleus may be considered to lose track of how it was formed, subject only to general conservation of the total energy, angular momentum, and parity established by the experimental conditions. The energy of excitation is quickly distributed among the constituents of the compound nucleus by intra-nuclear collisions, and the comparatively long lifetime of the compound nucleus may be interpreted as corresponding to the improbability of concentrating sufficient energy on a single particle to ensure its ejection, or of establishing a mode of charge oscillation giving rise to multipole radiation.

This state may subsequently decay through various different modes, namely emission of particles different from that incident, re-emission of the same (or equivalent) particle, or γ radiation. If each such mode has a probability w_i of decay per unit time, the state has an inherent spread in energy

$$\Gamma = \hbar \sum_i w_i \tag{2}$$

In the case of particle emission, the corresponding residual nucleus may also

be formed in an excited state, subject to decay by γ radiation to its ground state. If direct transition is forbidden, the radiation may involve several γ in cascade.

A study of the energy spectrum, yield per incident particle, angular distribution, etc., of nuclear radiation leads to information about the energy levels involved, and the coupling between these states.

Generally speaking, particle emission from an excited state of the compound nucleus, when energetically possible, is a much more probable mode of decay than is direct de-excitation by γ radiation, and the few cases where such radiation is observed at all are associated with severe restrictions on particle emission. Radiation associated with deuteron bombardment, for example, is almost exclusively associated with levels in the residual nucleus, whose radiation is "forced" by the primary process.

There remains an important class of proton-induced reactions in light nuclei* where no particle competition other than scattering of the incident particle is energetically possible up to several Mev; states in the nucleus resulting from proton capture can be investigated only by (1) proton scattering, (2) measuring capture γ radiation, or (3) using an entirely different reaction in which the nucleus in question appears as the residual nucleus.

Inspection of the energy level diagrams[1] will show that study of regions of excitation corresponding to the (p,γ) process by means of other reactions is usually afflicted with formidable experimental difficulties, such as

(1) unavailability of the necessary energy in present electrostatic accelerators,

(2) insufficient energy resolution in other types of accelerators,

---

* Proton capture resonances have been observed for $Z \leq 19$.

(3) unavailability of the appropriate target nucleus,

(4) problems associated with the detection of the emitted particles, especially neutrons.

The levels which have been thoroughly investigated, as shown in Reference (1) are largely fortuitous, and very few levels known have been investigated by more than one mode of excitation.

The reactions of the (p,γ) type which will concern us here are

$$C^{12} + H^1 \rightleftharpoons (N^{13}) \longrightarrow N^{13} + \gamma \qquad (3)$$

$$C^{13} + H^1 \rightleftharpoons (N^{14}) \longrightarrow N^{14} + \gamma \qquad (4)$$

These are the first two reactions in the Bethe "carbon cycle" of (p,γ) reactions responsible for energy production in the sun and hotter stars, which may be shown in a symmetric diagram:

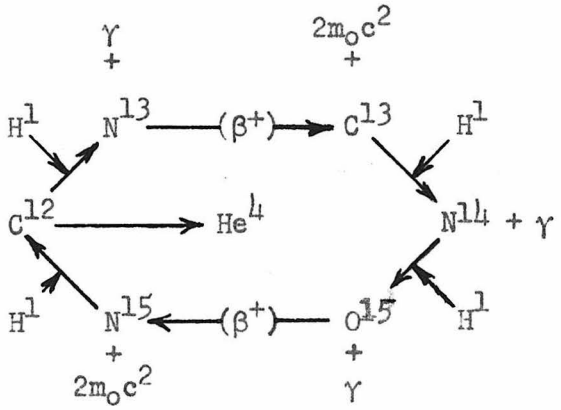

The last reaction $N^{15} + H^1 \rightleftharpoons (O^{16})^* \longrightarrow He^4 + C^{12}$ regenerates the C^{12}, and the net result of the cycle is a catalytic fusion of four protons into an alpha particle, with a net energy release of some 26 Mev per cycle.

Reaction (3) has been studied by several investigators[2 - 11]. The Q of this reaction, 1.92 Mev is quite low, associated with the strong binding of C^{12}. Resonances in N^{13} are known at 2.4 and 3.5 Mev, and appear in (p,γ), (p,p), and high energy (d,n) reactions. The Wisconsin group[12] has carried the (p,p) scattering up to proton energies of 4 Mev, and find

no further anomalies (at $\theta_{lab} = 164^{\circ}$).

Reaction (4), which is the primary subject of the present work, has been investigated until recently only at low energy[3],[4],[5],[11]. As it happens, the thick target yield from normal carbon (1.1% C^{13}) exhibits two steps of comparable intensity near proton energies of 500 kev, corresponding to the $C^{12}(p,\gamma)N^{13}$ resonance at $E_p = 0.45$ Mev and the $C^{13}(p,\gamma)N^{14}$ resonance at 0.55 Mev. The experimental problem of comparing these reactions will be discussed later. Reactions (3) and (4) are distinguishable by a marked difference in γ energy,* and in addition the residual nucleus N^{13} decays to C^{13} by a 10.1 minute, 1.2 Mev positron, while N^{14} is stable. The level at $E_p = 1.7$ Mev in $C^{12}(p,\gamma)N^{13}$ was first located by Van Patter[7], from the thick target γ yield, and confirmed by thick and thin target β^+ activity. Unpublished work by Fowler and Lauritsen at this laboratory with a thick sample of C^{13} enriched lampblack was continued above 1.3 Mev on the 3 Mev electrostatic accelerator by Day and Perry, who discovered a very sharp resonance in the vicinity of 1.76 Mev, and a broad contribution between the 0.55 and 1.76 Mev resonances. It was recognized that this strong resonance should appear superimposed on the broader resonance at 1.7 Mev due to C^{12}, even in a target of normal carbon. This was found to be the case by Day, using a thin lampblack target. He was in fact able to obtain angular distributions for both resonances separately[13].

The present work has involved preparation of thick and thin targets highly enriched in C^{13}, and an investigation of the energy levels and γ spectrum of N^{14} from proton energies of 0.4 to 2.7 Mev.

---

* ($Q = 1.92$ Mev for C^{12}, $Q = 7.56$ Mev for C^{13}).

II. APPARATUS AND EXPERIMENTAL SETUP

The 3 Mev electrostatic accelerator recently constructed at the Kellogg Radiation Laboratory provided a steady source of protons, continuously variable in energy, and maintained homogeneous to better than 0.1% by a 90° magnetic analyser of a double-focussing design[14]. Current collected on the analyser exit slits was used to regulate the accelerator potential by modulating the corona drain from the terminal. Ashby and Hanson[15] describe such a "Corona Triode". We have used a design giving a transconductance of about 70 μa / kilovolt. This equipment has been described in detail elsewhere[16].

An auxiliary pump and cold trap between the analyser and target chamber helped minimize contamination of the targets by normal carbon and oxygen from pump oil vapor.

The target chamber was a T-shaped assembly of 1/2" inside diameter x 1/32" wall brass tubing, with a quartz window at the joint for inspection and alignment of the beam. The target support was affixed to one end of a drill rod passing through a sliding O-ring seal in a brass plug fitting into one end of the transverse leg of the T; the plug was also sealed to the tube by means of an O-ring. This arrangement made it easy to align (and reproduce) the target position, and to change targets rapidly.

The basic detection unit was a system of three Geiger tubes* of 30 mg/cm^2 glass wall and a sensitive region 3/4" in diameter x 3 1/2" long. These were placed in a geometrical arrangement standardized at this laboratory, shown in Figure (1). Secondary electrons produced in the aluminum converter which pass through both the front counter and either one of the two rear counters are registered by standard coincidence circuits as a coincidence

---

* Made by Radiation Counter Laboratories.

count. The spectrum of the initial γ radiation may be inferred by studying the reduction in coincidence rate as a function of the thickness of aluminum absorber placed directly in front of the rear counters. Application of this method will be discussed later.

For the thin target and absorption curve work, the counter system was enclosed in a special lead shield. A receptacle for a standard ThC" γ source permitted periodic checks on counter operation. The preliminary thick target measurements were carried out in the setup previously used by Day and Perry for angular distributions[13]. The arrangement differed from that described above only in that there were two separate sets of coincidence systems, and the entire system of target chamber and counters was enclosed in a large aluminum-lined house of lead bricks. The use of both sets simultaneously permitted securing greater statistical accuracy without increasing the time of bombardment.

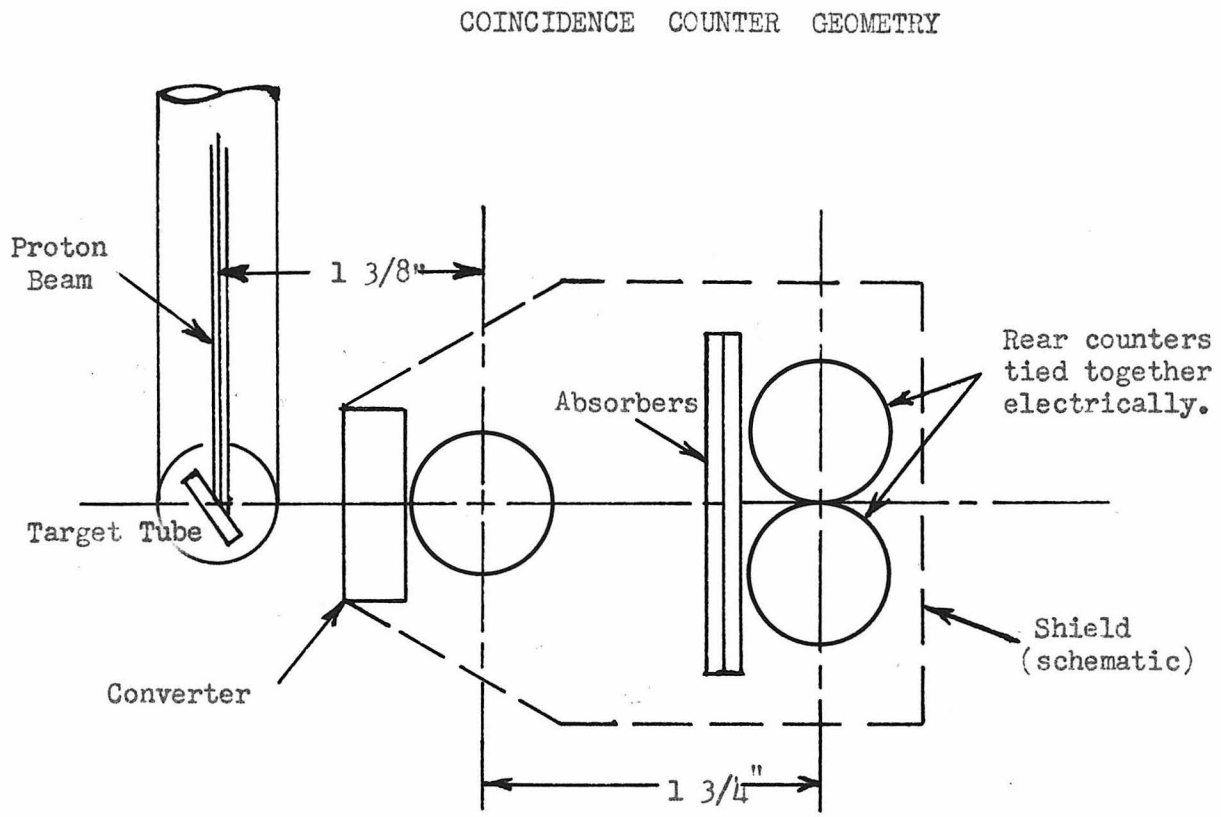

Figure 1. Showing semi-schematically the coincidence counter geometry used. The absorbers are held in place directly in front of the rear counters. The ratio of coincidence counts with no absorber to front counts is 0.30 ± 0.03 for three to nine Mev gamma radiation.

III. PREPARATION OF THE TARGETS

The original thick target used by Fowler and Lauritsen was unsatisfactory in that the copper backing used gave a strong γ yield at the higher proton energies available with the larger accelerator. A new target blank was made from a strip of Sterling silver by milling a 3/8" diameter recess from one side to within .010" of the other, and soldering it to a brass sleeve. To secure a sufficiently durable target of this size, it was found necessary to wet the lampblack with a dilute solution of shellac in alcohol. After evaporation of the solvent, the target material could be pressed into a pellet within the silver support.

Preparation of the thin targets with a previously unattained thinness and uniformity was somewhat more complicated, and will be described in more detail. It was clear that thin soot films were quite non-uniform and gave rise to severe straggling in proton energy loss, and in addition could not be made thin enough for convenient investigation of narrow resonances. Attempts to deposit films of carbon by evaporation of the matrix from a colloidal suspension of graphite were unsatisfactory. So far as I know, no attempt at vacuum evaporation of carbon, as from an electric arc, has had any success at all.

G. C. Phillips[17] prepared thin targets of normal carbon by "cracking" benzene vapor on thin silver foils. In view of this, an attempt was made at this laboratory to crack other hydrocarbons, starting with methane. Films were obtained readily by passing current through .005" tantalum strips in about 1/2 atmosphere of illuminating gas. On the metallic surface, a thin film was quite invisible, but was detected and measured by the γ yield at the 1.76 Mev proton resonance due to the 1.1% C^{13} present. By comparison with a soot target, these films were shown to be nearly pure carbon, within the statistical accuracy attainable (5%) on such a weak source. The 1.76 Mev

resonance was very convenient to use, since the coincidence rate from the 3.5 Mev radiation from N^{13} could be attenuated markedly compared with the 9.2 Mev radiation from N^{14}, and since the targets were much thicker than the width of that resonance (about 2 kev), the yield was independent of target thickness. (See Equation 15).

Carbon enriched in C^{13} was found to be available* in the forms $BaCO_3$, KCN, and CH_3I, of which the methyl iodide appeared by far the most promising. Preliminary experiments with normal CH_3I indicated that carbon films were indeed formed by cracking the vapor directly, but that a tendency to "blister" and peel off observed with methane, was more serious, and the voluminous production of I_2 vapor was a nuisance in the cracking chamber, as it rapidly obscured inspection of the Ta strip.

Chemical methods of removing the iodine from the methyl iodide were considered, of which the most direct seemed to be hydrolysis or alcoholysis of a Grignard reagent prepared from the methyl iodide sample, according to the reactions

$$CH_3I + Mg \longrightarrow Mg(CH_3)I \text{ (Grignard reagent)}, \qquad (5)$$

followed by

$$Mg(CH_3)I + H(OH) \longrightarrow MgI(OH) + CH_4 \text{ (Hydrolysis)} \qquad (6)$$

It appeared however, that an elaborate setup would be required to handle the precious enriched material without appreciable loss or contamination or dilution (by exchange of carbon if alcoholysis used instead of hydrolysis). An order was placed for a drop of methyl iodide containing 0.1 grams of actual C^{13} at an absolute concentration of 61 atom %, and the direct use of CH_3I vapor studied in a "cracking tower" constructed for the purpose, shown in Figure (2).

---

* From Distillation Products Industries, Eastman Kodak Company.

A tantalum strip 0.002" x 1/2" x 3" is clamped at its ends to two heavy current leads of 1/4" copper rod, one of which is soldered to a brass plug, and the other passes through Koroseal packing in a modified Imperial fitting, which provides both electrical insulation and a vacuum seal. The chamber proper is a pyrex tube, sealed by O-rings as shown. The lower valve assembly was made to fit directly on a laboratory vacuum system. The method developed for handling the hydrocarbon phases is shown semi-schematically in Figure (3). Pyrex was used throughout, and convenient condensing tubes were made by shellacking neoprene stoppers into side-arm test-tubes. The system was assembled with Koroseal tubing. CH_3I is quite active, attacking rubber (and skin) readily, but the simple apparatus described worked so well in tests with normal CH_3I that it was used with the enriched material without further refinement. It was necessary to seal an iron plug in glass, and include it in the inner-sealed container in which the enriched material was vacuum-packed, so as to admit the vapor directly into the evacuated chamber, by breaking the inner seal.

Transfer of the material was simply effected by condensing the vapor in the traps, and by allowing it to vaporize and enter into the chamber previously evacuated. A flask of liquid Nitrogen was used as the refrigerant, and sufficient vapor pressure was attained by warming the trap gently by cupping it in my hand.

The straggling of protons observed with the first films made was nearly eliminated by careful polishing of the tantalum, the balance being on the order of "natural" straggling expected from the nature of the energy-loss process since the carbon is presumably laid down atom-by-atom, and should conform to the surface on which it is "cracked". The polished strips were carefully cleaned in alcohol and then in distilled water. No difference was detected between films made on Ta outgassed in a hard vacuum (10^{-5} mm Hg) and those "vacuum-cleaned" by a glow discharge while the chamber was being evacuated

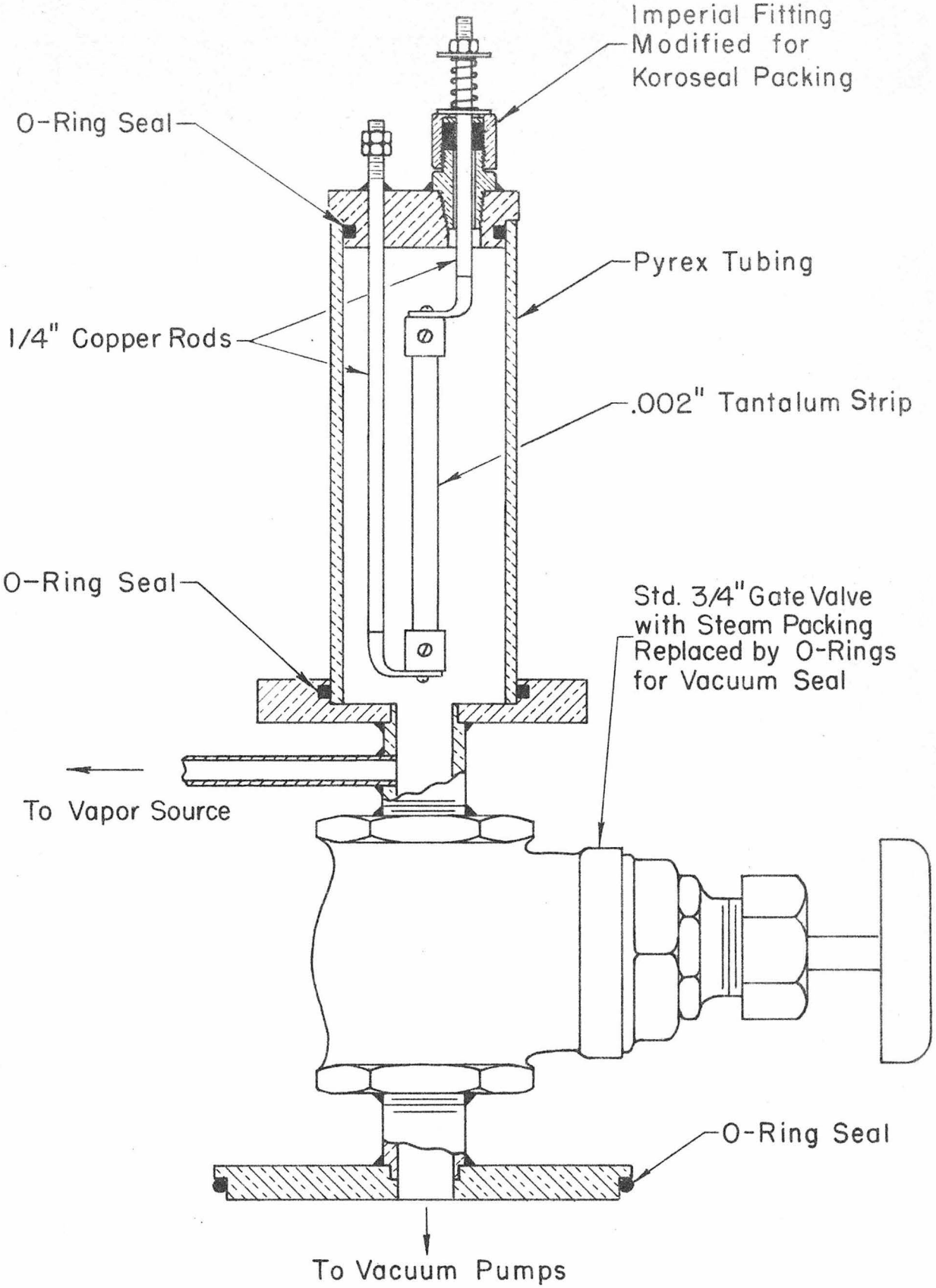

CRACKING CHAMBER

FIG. 2

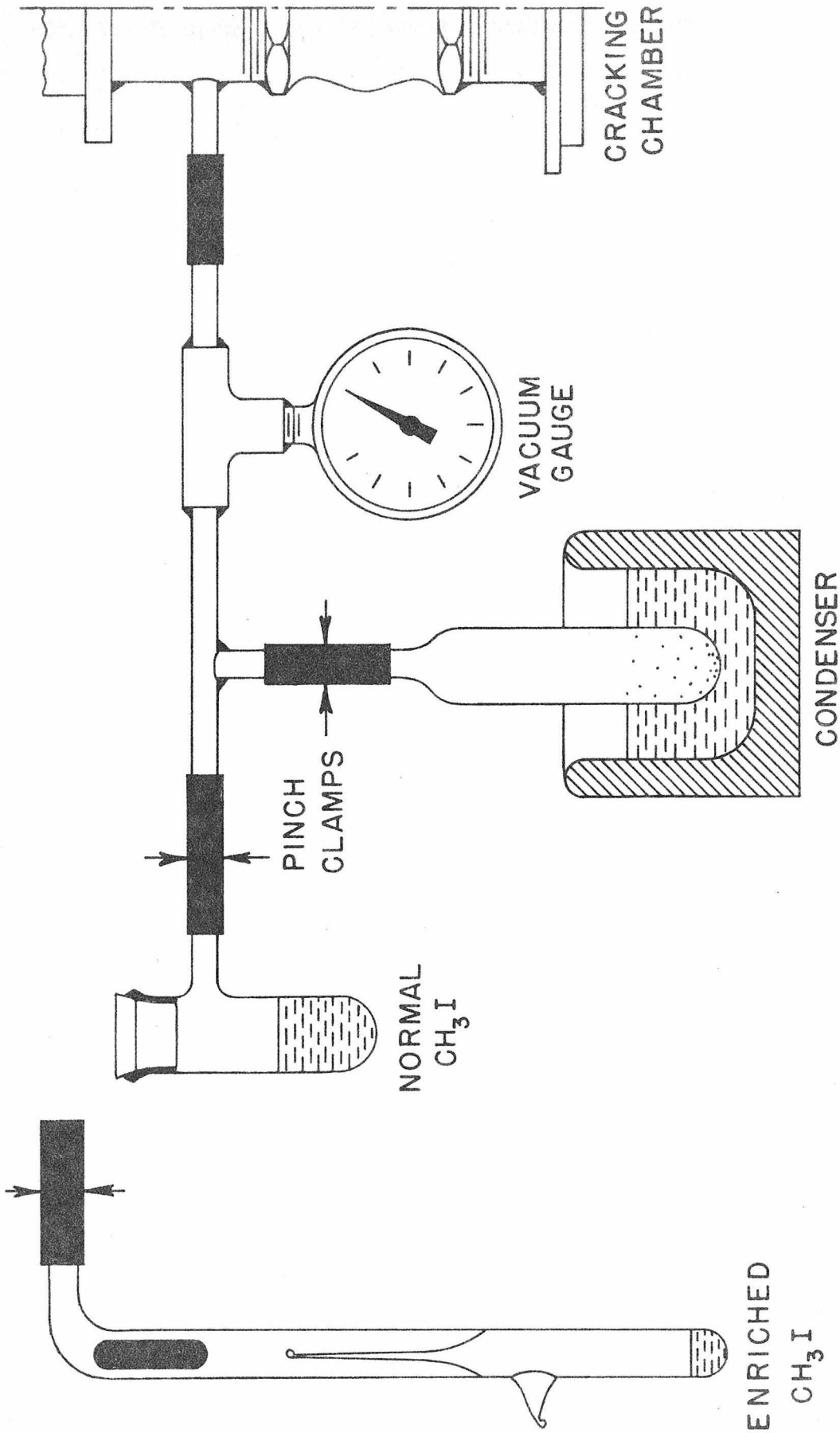

VAPOR TRANSFER SYSTEM

FIG. 3

with the forepump alone (to about 5 microns). Since the latter process was easily arranged by connecting the secondary of a "neon" transformer across the pyrex tube, no further attempt at high vacuum outgassing was made. A cycle of operation of the chamber is described:

(1) Close off supply tube and evacuate chamber and trap. Produce glow discharge.

(2) Immerse supply tube in refrigerant until CH_3I frozen, then pump off any air introduced with the sample.

(3) Seal the trap, and close valve to pump.

(4) Allow the CH_3I to melt and expose it to the evacuated chamber, until the vapor pressure reaches the desired value (normally 3 or 4 in. Hg).

(5) Seal the supply tube.

(6) Cracking proceeds when the Ta strip is heated to 600 to 650 $^{\circ}C$ (bright orange) and is allowed to continue for 10 to 20 seconds, depending on the pressure and film thickness desired. For the strip described, this required 70 to 90 amperes from a current transformer.

(7) The trap is now opened to the system and immersed in the refrigerant, and in a few seconds virtually all the vapors (except H_2) have condensed in the trap, which is then sealed.

(8) Air is admitted and the chamber opened and cleaned (of iodine crystals), and a new strip put in place and the chamber evacuated as in (1). It is now possible to run several cycles, using the reclaimed vapors in the trap, without opening the supply tube. Indeed, the H_2 (together with some CH_4) can be pumped off as in (2), while the rest is frozen.

It was found that the majority of the iodine present was cracked free

from the methyl group during the first cycle. Substantial carbon films could be obtained from the residual vapor with very little iodine generation. Apparently a reaction like $2CH_3I \rightarrow I_2 + C_2H_6$ can proceed at a slightly lower temperature than the cracking of the C:H bond to release carbon. I_2 vapor was observed at about 500 °C (dull red), when no carbon was deposited.

Trouble was encountered early in the investigation with blistering of the carbon film from the tantalum, and appeared to be associated with high rates of deposition and with buckling of the Ta strip due to thermal expansion. To minimize this effect, vapor pressures less than 4" Hg were used; a spring was attached to the copper rod above the vacuum joint to maintain tension; and the strip was heated and cooled as slowly as possible. The enriched targets made were free from the effect, though part of one did blister during subsequent handling. However, by encouraging blistering, it is possible to remove sections intact as large as 5 x 5 mm, which should be of interest when an unsupported target is desired. In appearance these "foils" greatly resemble thin beryllium foils. It is hoped to investigate this technique further, in the near future.

Several strips of "C^{13}" films on tantalum were made in the above manner, of which the most satisfactory were 16, 8, and $<$ 1 kev thick, as measured by the resonance at 1.76 Mev.

It is of interest to calculate the amount of carbon in such films. The stopping cross-section for 1.76 Mev protons on carbon is $\varepsilon = 3.32 \times 10^{-15}$ ev-cm^2. Then, assuming the film had the density of graphite, $\rho = 2.25$ gm/cm^3, and using $N_a = 6.02 \times 10^{23}$ mol^{-1}, and an effective mol weight W = 12.61 gm/mol in the relation

$$\Delta E = N_a(\rho/W)\,\varepsilon\, t \qquad (7)$$

we obtain a thickness of 4.5×10^{-5} cm or 0.45 microns for an energy loss of 16 kev. This is then a surface density of 100 μg/cm^2, and it requires about 100 μ mol of carbon to cover such a strip. The volume of the chamber

is about 100 cm^3, and at 1/10 atmosphere contains 450 μ mol of carbon in the vapor. Thus about 20 percent of the carbon atoms present are used in making such a film. In addition, the 0.1 gm of C^{13} represents 7.7 millimols, so a great many such targets could be made even if each chamberful were "used" but once.

Richardson[18] has developed a similar method for producing thin films by cracking. He employs a thick Nickel disk on a quartz support, and heats it by means of an induction furnace. He states that the use of high vacuum is essential, to prevent formation of NiO. He found the degree of heating more critical than reported here, and got no deposit at yellow heat, as the metal evaporates and NiI_2 is formed. Nickel was chosen since it is employed in large-scale cracking of heavy hydrocarbons to lighter fractions. It is not clear that any strictly catalytic action takes place, unless Ta happens to do the same thing. In view of our rough agreement on the temperature at which the cracking takes place, and the very different physical properties of Ni and Ta, such action seems doubtful. It is gratifying that the considerably simpler methods employed here give highly satisfactory results. Possibly Richardson's method would be the more useful for making thicker targets, but the principal interest for nuclear bombardment experiments lies in producing very uniform thin targets, as were employed here.

IV. THE EXCITATION FUNCTIONS

Before presenting the excitation functions, it will be convenient to collect here the mathematical expressions for the shapes expected in the excitation function (Yield as a function of energy) for a general resonance[19]. It will be assumed that the resonance is characterized by a (constant) width at half-maximum Γ, and a cross-section σ_R at the resonance energy E_R. For a single resonance,

$$\sigma(E) = \sigma_R \frac{\Gamma^2/4}{(E - E_R)^2 + \Gamma^2/4} \qquad (8)$$

Then if the bombarding beam suffers an energy loss ξ in traversing the target, the yield

$$Y = \int_{E-\xi}^{E} (\sigma/\varepsilon_d)\, dE, \tag{9}$$

where ε_d is the "stopping cross-section" per disintegrable nucleus in the target. Since ε_d and ξ vary slowly with energy, for a reasonably narrow resonance we can evaluate them at the resonance energy and carry out the integration in Equation (9) analytically, and find

$$Y = \frac{\sigma_R \Gamma}{2\varepsilon_d}\left[\tan^{-1}\left(\frac{E - E_R}{\Gamma/2}\right) - \tan^{-1}\left(\frac{E - E_R - \xi}{\Gamma/2}\right)\right]. \tag{10}$$

It can readily be shown that Equation (10) has a maximum at $E = E_R + (1/2)\xi$ given by

$$Y_{max}(\xi) = \frac{\sigma_R \Gamma}{\varepsilon_d} \tan^{-1}\left(\frac{\xi}{\Gamma}\right) \tag{11}$$

and an apparent width at half maximum

$$\Gamma' = (\Gamma^2 + \xi^2)^{1/2} \tag{12}$$

In the case of a thick target ($\xi >> \Gamma$), the second term inside the brackets in Equation (10) $\longrightarrow +\frac{\pi}{2}$. It is sometimes convenient to interpret the "bell-shaped" function (10) as the difference between two infinitely thick target yield functions, one centered at $E = E_R$, the other displaced to higher energy by the target thickness ξ. It follows from Equation (11) that

$$Y_{max}(\infty) = \frac{\pi}{2}\frac{\sigma_R \Gamma}{\varepsilon_d}, \tag{13}$$

and that $$\frac{Y_{max}(\xi)}{Y_{max}(\infty)} = \frac{2}{\pi}\tan^{-1}\left(\frac{\xi}{\Gamma}\right). \tag{14}$$

Another relation involving the target thickness computes the average energy loss from the area under the excitation curve:

$$A(\xi) = \int Y\, dE = \frac{\pi}{2}\frac{\sigma_R \Gamma}{\varepsilon_d}\xi = Y_{max}(\infty)\cdot\xi \tag{15}$$

This result can be shown[20] to be independent of the homogeneity of the beam and the exact shape of the thin target yield.

The excitation function obtained with the C^{13} enriched lampblack target is shown in Figure (4). Since N^{14} produced is excited to about 9 Mev while N^{13} is excited to about 3 Mev, an 0.150" aluminum absorber was employed in the coincidence setup described previously.* This thickness of absorber reduced coincidence counts from N^{13} radiation to a negligible level, while attenuating 9 Mev radiation only about 50%. The coincidence excitation function shown is thus a measure of the high energy yield only. The bombardment was carried down to 600 kev, as low as it was convenient to operate the accelerator. The low energy data was in agreement with the data obtained by Fowler and Lauritsen on the 1 1/2 Mev accelerator for proton energies of 400 to 1200 kev. The two sets of data were normalized at 700 kev, as shown.

The strong sharp resonance at 1.76 Mev manifests itself as an abrupt "step". The "rise above resonance" observed in the low energy data is seen to exhibit the general features of an extremely broad resonance centered near 1.3 Mev, and extending over several Mev. In this case the assumptions underlying Equation (10) do not apply.

A small bump appears at 1.16 Mev, and is more marked in the front counter data (not shown), as is a similar bump at 2.1 Mev which is not resolved in the coincidence curve at all. These weak resonances thus give much softer radiation than do the principal resonances.

Data is given in Table I for the relative thick target yield of the three principal resonances:

---

* Absorption equivalent to 0.020" of aluminum provided by the counter walls has been included in labelling the drawing "0.170" Al absorber".

FIG. 4

$C^{13}(p,\gamma)N^{14}$

Thick Target Yield

1 ½ MEV GENERATOR

3 MEV GENERATOR

x 5

COINCIDENCE COUNTS / MICROCOULOMB

40
35
30
25
20
15
10
5

PROTON ENERGY IN MEV

0.6 0.8 1.0 1.2 1.4 1.6 1.8 2.0 2.2

YIELD MEASURED AT 90°
244 μ COULOMBS EACH POINT
0.170" Al ABSORBER

TABLE I

E_R	γ_1 (front)	C (coinc)	C/γ_1	E_{ex}	$Y_{max}(\infty)$
0.55	1	1	1	8.1	1
1.3	1.9	1.8	.95	8.8	1.8
1.76	1.67	2.2	1.3	9.2	1.5

It is apparent from the C/γ_1 column and the attenuation of secondaries from softer radiation in the coincidence measurements, that (a) the radiation at 1.76 is harder than that at 0.55 Mev, and (b) the radiation from the broad resonance may contain softer components. In the values given in Table I for C and γ_1 (counts), account has not been taken of the Geiger tube efficiency (counts/quantum), which increases with quantum energy. In the following, it will be assumed that this efficiency is accurately given by Fowler's expression*

$$0.70\ (E_\gamma)\%, \text{ for } E_\gamma \text{ in Mev} \qquad (16)$$

valid at least above 2 Mev, for the counters employed with aluminum converters.

Allowance for this difference and the different attenuation in the absorber is sufficient to reconcile the front and coincidence rates at the 1.76 Mev resonance if the radiation there and at 0.55 Mev is primarily of the available energy E_{ex}. Conclusion (b) is supported since C/γ does <u>not</u> increase with E_{ex}. It may be pointed out here that if a state of given excitation decays by cascade, or even in several branches of cascade, the several quanta of lower energies are detected with correspondingly lower efficiency, so that the single counter measures the number of primary <u>disintegrations</u>, independent of the details of the spectrum. Relative values of γ_1/E_{ex} are given in the column of Table I labeled $Y_{max}(\infty)$.

With the original thick target, Day and Perry determined the location

---

* Compare Reference (19), p.264.

of the sharp resonance as 1754 ± 3 kev, and its width as 2.5 ± 0.5 kev. A later value of 1757 ± 3 kev on the same target may have been shifted up by a layer of contamination deposited by the beam. It was hoped to secure more precise values with the more highly enriched and uniform targets, but difficulties with regulation of the magnetic analyzer arose and made it difficult to validate a more precise determination of the energy. A sharper value for the width will be discussed below. It is planned to carry out this important experiment as soon as the electrostatic analyzer now being tested can be calibrated. Indeed, the resonance should prove very useful as a standard itself, as it is believed the sharpest proton resonance now known in the light nuclei ($Z \leq 10$), and its high energy radiation makes detection convenient. We shall continue to refer to it here as the "1.76 Mev resonance".

Sections of several C^{13}-coated tantalum strips were selected and their "profiles" examined by means of the sharp resonance. A 16 kev target particularly free from straggling was used in most of the following work.

A preliminary survey was made with one such "16 kev" target, in roughly 15 kev steps from proton energies of 0.7 to 2.2 Mev, using only 0.050" aluminum absorber*, with the current integrator set to accumulate 111 microcoulombs. The coincidence curve is shown in Figure (5), and brings out the weak resonances at 1.16 and 2.10 Mev. By the use of Equation (12) and the known variation with energy of the stopping cross-section for carbon to find the thickness at other energies of a target 16 kev at 1.76 Mev, the widths were found to be about 5 kev at 1.16 Mev and 45 kev at 2.10 Mev. In addition, the broad resonance centered near 1.3 Mev is seen to be rather unsymmetrical. Some preliminary absorption curves were made, confirming the soft nature of the radiation at the weaker resonances.

---

* Added absorber -- see footnote Page 17.

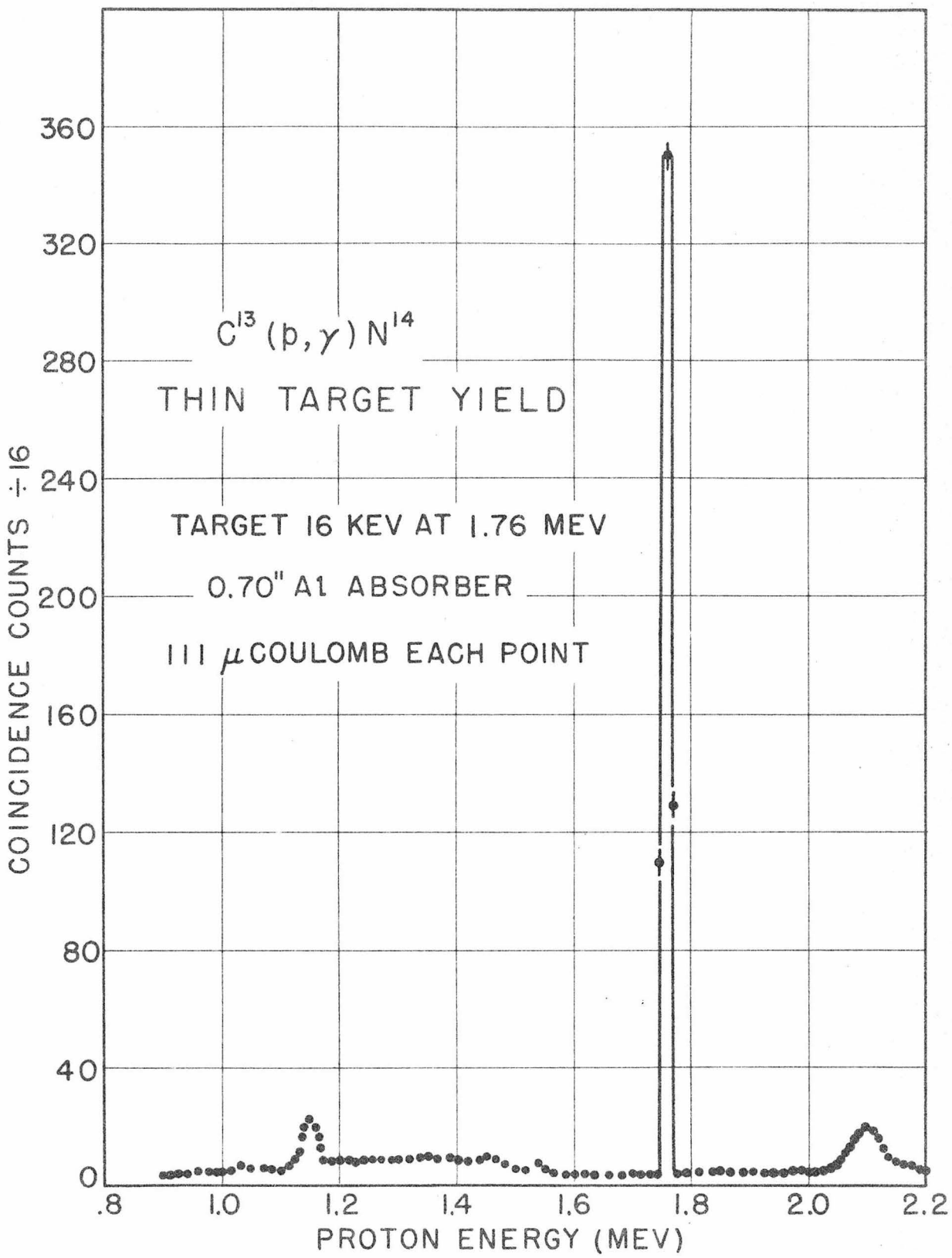
$C^{13}(p,\gamma)N^{14}$
THIN TARGET YIELD
TARGET 16 KEV AT 1.76 MEV
0.70" Al ABSORBER
111 μ COULOMB EACH POINT
COINCIDENCE COUNTS ÷16
360
320
280
240
200
160
120
80
40
0
.8
1.0
1.2
1.4
1.6
1.8
2.0
2.2
PROTON ENERGY (MEV)

FIG. 5

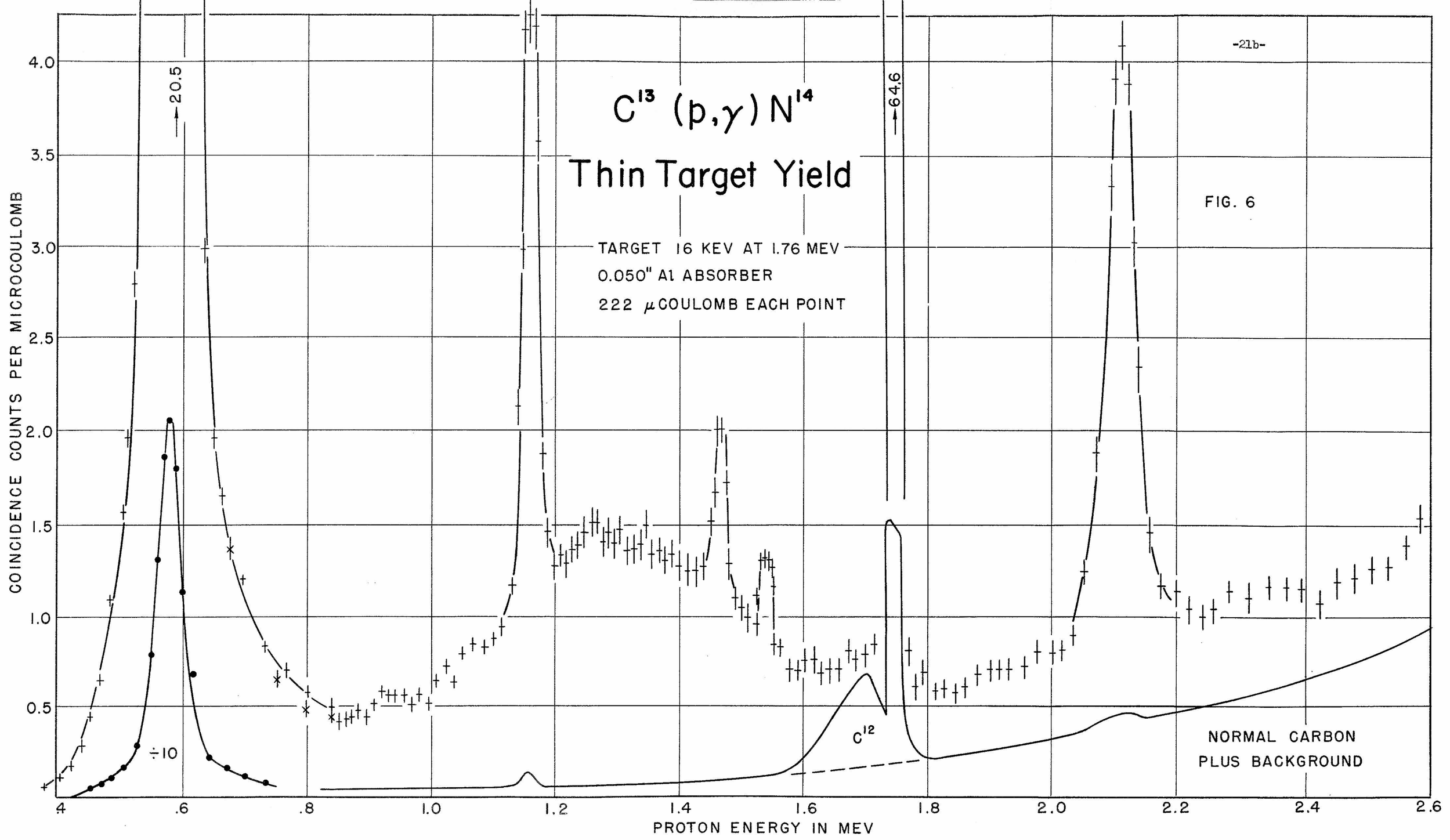
$C^{13}(p,\gamma)N^{14}$
Thin Target Yield
TARGET 16 KEV AT 1.76 MEV
0.050" Al ABSORBER
222 μCOULOMB EACH POINT
20.5
64.6
÷10
C^{12}
NORMAL CARBON
PLUS BACKGROUND
COINCIDENCE COUNTS PER MICROCOULOMB
PROTON ENERGY IN MEV
4.0
3.5
3.0
2.5
2.0
1.5
1.0
0.5
.4
.6
.8
1.0
1.2
1.4
1.6
1.8
2.0
2.2
2.4
2.6

FIG. 6

With 0.030" absorber, to suppress only the annihilation quanta from the N^{13} positron decay, a complete excitation curve was run, with twice the charge and more closely spaced intervals. As is seen in Figure (6), P.21b, a good deal of structure was revealed. Attention is called to the scale, on which the 1.76 Mev yield is 16 times the height of the paper.

The regions of the principal resonances were repeated, and examined with thinner targets. Successive runs were made with a large overlap, and the operation of the counters checked periodically with a standard ThC" source. Background readings were taken by bombarding a 20 kev normal carbon film deposited on tantalum in the same manner as those enriched in C^{13}. The two targets were mounted on opposite sides of the target support, which could be rotated, so that background checks were made without delay or other changes in the system. The background of coincidences was small. Above 2 Mev, a large amount of very soft radiation from the tantalum produced many singles counts, giving rise to accidental coincidences. This effect was suppressed by the addition of an extra 1/8" lead converter, without affecting appreciably the high energy radiation.

The data has been plotted showing the statistical error $\pm \sqrt{n}$ for n counts, which becomes important when working with the small yields studied here.

The smooth background curve is also shown. The normal carbon target was bombarded in the regions of the resonances presumed due to C^{13} for a sufficiently long time to insure statistically significant values of the normal yield. The assignment of the resonances at 1.16 and 2.10 Mev was confirmed in this manner. In between background checks were merely observed to be consistent, and were generally negligible. The 1.70 Mev resonance due to C^{12} is clearly shown in the "background" curve.* Because $\Gamma(C^{13}) \ll \xi \ll \Gamma(C^{12})$

---

* The enriched (61%) C^{13} target is of course impoverished (39%) in C^{12}, while the "background" is taken with a normal (98.9% C^{12}) fraction.

(compare Equation 14), the sharp C^{13} peak stands out clearly and indicates the width and uniformity of the target. The 0.55 Mev resonance was examined using the "Mass Two" (H_2^+) component of the beam, and the data overlapped with the Mass One data for 200 kev, justifying its use free from serious contamination with deuterons.*

Because of their very small yield, the resonances at 1.47 and 1.55 Mev could not be definitely assigned to C^{13} by comparison with normal carbon. The region was examined with a target half as thick, and the reductions in yield and observed width favor values of about 16 and 6 kev for the widths if that assignment <u>is</u> correct. However the region was also examined with a "normal" target, and a bump about 1/5 as large found at 1.55 Mev. A somewhat larger bump was found about 60 kev below 1.47 Mev. A fresh "normal" target showed no effect at all. An attempt was made to identify possible impurities. The light nuclei are ruled out by their well known excitation functions, as is phosphorus, the only impurity anticipated from the chemistry of preparing the enriched material,** whose yield function[21] does exhibit resonances in this region, but also shows stronger resonances which we did <u>not</u> observe.

Blank (and negative) runs were also made on Ta strips exposed to CS_2 and to I_2 vapors in the cracking chamber. Iodine would hardly be expected to admit proton resonances, because of the forbidding barrier factor for $Z = 53$. It would not be surprising to find a "trace" of iodine trapped in the target, however. One of these targets was used in scattering experiments [22] and a small unidentified bump appeared in the analyzer $B\rho$ spectrum just before the strong Ta rise. Interpretation as scattering due to $_{53}I^{127}$ is

---

* The gamma yield following (d,p) and (d,n) reactions in carbon would be at most only a few percent of the (p,γ) yield if the beam had a normal isotopic content of deuterium.

** D. W. Stewart (Eastman Kodak Company), private communication. I also understand that our "normal methyl iodide", although also made by Kodak, is made by a different process than the enriched material.

plausible, in which case the intensity relative to carbon scattering would imply an iodine contamination of not more than 0.5%*.

In view of (a) the weak intensity of these 1.47 and 1.55 Mev peaks,

(b) the difficulty of unequivocal assignment, and

(c) the complexity of interpreting even the much stronger resonances,

these two resonances will not be treated further.

The target enrichments were checked by the yield at 1.76 Mev and found to be 64.6 ± 3%, so it seems safe to take DPI's value of 61% as exact. Identical yields were obtained from normal films and normal lampblack, so the stopping power of the target may safely be taken as that for pure carbon.

The principal resonances were examined with several targets and the yields and observed widths reconciled by the use of Equations (12), (14), and (15) to give values for the widths, which are tabulated in Table II:

TABLE II

E_R (Mev)	0.55	1.16	1.3	1.76	2.10
Γ (kev)	32.5	6	~450	2.1	45
Error (kev)	± 1	± 2	-	±0.2	± 3

In the case of the 1.76 Mev resonance, a target was prepared for which the (integrated) width was 0.5 kev. The 1.3 Mev resonance is so broad that its half-width is a function of energy, and not very well defined. Also, it will be noticed that the detailed excitation function shows some non-resonant yield above 1.8 Mev, which must extend to somewhat lower energies, and how this may be related to the "tail" of the broad state is not certain.

The lowest resonance was examined in somewhat greater detail, to find $Y_{max}(\xi)/Y_{max}(\infty)$, and to pursue preliminary evidence that the width was

* Ward Whaling, private communication.

rather less than the 40 kev previously reported.[5] The resonance is somewhat unsymmetrical (Γ is not a constant in the dispersion formula, due to the rapid variation of the penetration factor at low energies), so that interpretation plays a part in the value given for Γ. The excitation function for this resonance was studied with the same target at three angles to the beam, and the target profiles were measured at 1.76 Mev for each position, so that knowledge of the target thicknesses was not dependent on accurate measurement of the target angle. At both 0.55 and 1.76 Mev, the target thickness was calculated by integrating the yield function and using Equation (15). The thickest target used was sufficiently thicker than the resonance width that advantage could be taken of the "infinitely" thick target yield function, Figure (4), which was normalized in magnitude to fit the thickest "thin" target data at the point of inflection and below. $Y_{max}(\infty)$ was taken as the value at 700 kev.

Finally, the interpretation of a thin target yield as the difference of two thick target yields mentioned in connection with Equation (10) -- which follows from manipulation of the limits of integration in Equation (9) and does not depend on the integrand having a particular form -- was used as a check on target thicknesses, by determining graphically the shift of the thick target functions required to "explain" the thin target functions. These results are shown in Figure (7), where the symbols X denote values calculated graphically for the positions shown (dashed lines) of the displaced thick target yield function. The internal consistency of these procedures is shown in Table III .

TABLE III

Target angle θ	0	60°	75°	Target Widths
Integrated $\xi_{1.76}$	15.5	29.2	57.9 kev	
$\xi_{1.76}(0°)/\cos\theta$	(15.5)	31	58 kev	
2.3 x $\xi_{1.76}$	35.7	67	133 kev	
Integrated $\xi_{0.55}$	32	68	134 kev	
Shift for best fit	35	66	130 kev	
$Y_{max}(\xi)/Y_{max}(\infty)$	0.50	0.71	0.90	
Observed Γ'	48	70	133 kev	
$\Gamma = \sqrt{\Gamma'^2 - \xi^2}$	32.5	-	- kev	Resonance
Γ from Equ. (14)	32	33.4	- kev	Width
Final Result:	Γ = 32.5 ± 1 kev at E_R = 0.554 ± .002 Mev.			

The value for the resonance energy obtained from subtracting half the target thickness from the energy at the maximum (for the thinnest target) is 555 ± 2 kev, while that from fitting the thick target yield function is 552 ± 3 kev. The latter is more uncertain because during the long bombardment with Mass Two, a layer of contamination built up on the target. The low energy data was shifted by an amount calculated from the shift necessary at 1.76 Mev (2.3 is the ratio of stopping cross-section at 0.55 and 1.76 Mev). We are thus in complete agreement with Fowler's value[5] of 0.554 ± .002 Mev, but conclude that the resonance width is some 20% smaller than his value of 40 kev.

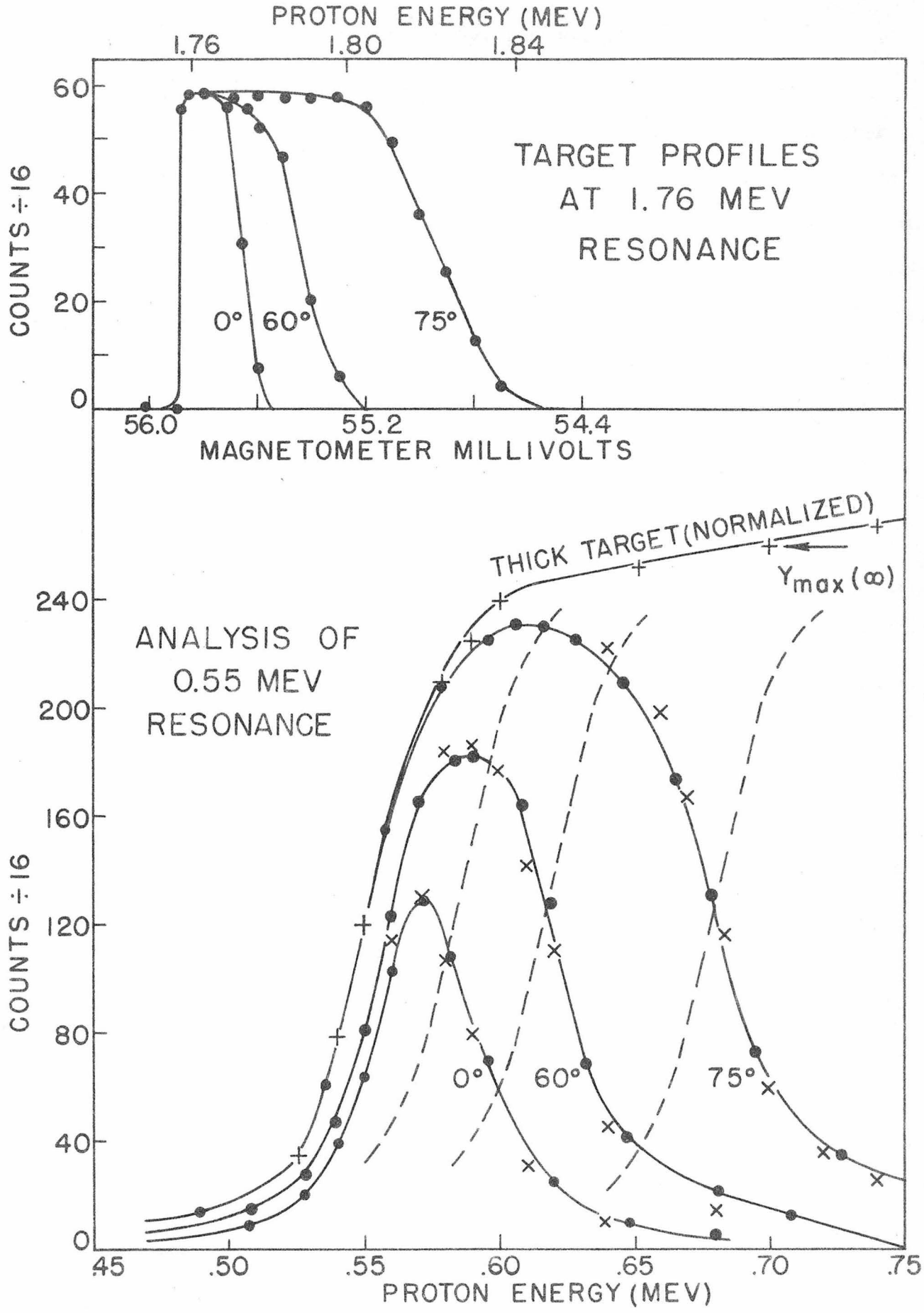
PROTON ENERGY (MEV)
1.76
1.80
1.84
60
40
20
0
COUNTS ÷ 16
TARGET PROFILES
AT 1.76 MEV
RESONANCE
0°
60°
75°
56.0
55.2
54.4
MAGNETOMETER MILLIVOLTS
THICK TARGET (NORMALIZED)
$Y_{max}(\infty)$
ANALYSIS OF
0.55 MEV
RESONANCE
240
200
160
120
80
40
0
COUNTS ÷ 16
0°
60°
75°
.45
.50
.55
.60
.65
.70
.75
PROTON ENERGY (MEV)

FIG. 7

V. THE ABSORPTION CURVES

A study of the radiation from each of the principal resonances was made by measuring the coincidence counting rate as a function of absorber placed between the counters. The absorbers were held in place directly in front of the rear counters by a phosphor bronze strap spring. These "absorption curves" were carried below 1% transmission until background, accidental coincidences, and statistical fluctuations became serious. The front counter was used as a monitor on constancy of the radiation from the target. Background readings were measured with 0.700" aluminum absorber in place and the radiation present, to include the effects of accidental coincidences. The data was corrected for this background and normalized to unit transmission for zero (added) absorber, and plotted as discussed below.

A "master curve" for absorption of secondary electrons from γ radiation, applicable to this geometrical arrangement, has been prepared by Schardt[23] based on Reference 5 and an experimental study of several well known γ rays. A copy of this set of curves is reproduced in Figure 8 on the same semi-logarithmic scale as are shown the $C^{13}(p,\gamma)N^{14}$ data in the following Figures 9 - 12.

Radiation of a single energy is expected to exhibit the shape of the interpolated "master curve". If the radiation consists of several γ's of different energy, the composite curve could be calculated. If we call the transmission function of absorber thickness for a particular energy $T(x,E)$, then the composite function for radiation composed of fractions f_i of γ's of energy E_i will be

$$T(x) = \frac{\sum_i T(x,E_i)\ f_i E_i}{\sum_i f_i E_i} \qquad (17)$$

where the factors E_i arise from the linear dependence of Geiger tube efficiency on energy given by Equation (16). As an example, if a 9 Mev state decays by

6 and 3 Mev γ's in cascade, we would expect a transmission curve obtained from the (algebraic) sum of T(x,6) drawn to intersect the (logarithmic) axis at 0.67 and T(x,3) intersecting at 0.33. In analysis of unknown mixtures, the process is reversed. The high energy tail of the experimental curve is fitted to the master curve,* and the fitted curve drawn across to intercept the axis. The intercept gives the fraction of counts due to that energy. Then the (algebraic) difference is replotted, and in principle the procedure could be repeated. Unfortunately, if proper account is taken of the probable errors of the data, and those inherent in such graphical solutions, the procedure outlined cannot be carried very far. In addition, the linear dependence of detection efficiency on energy causes high energy quanta to mask the low, and in the case of complex radiation, involving more than two γ's in cascade, or involving competing branches of decay, the above procedure does not yield very satisfying results. This appears to be the case for $C^{13}(p,\gamma)N^{14}$: both branching and cascades occur.

In Figure 9, the absorption curve for the 1.3 Mev resonance is shown. The tail has been fitted by a curve corresponding to 8.8 Mev, the energy of excitation. For thin absorbers, the curves break away, and the difference is seen to correspond to much lower energy, suggesting the possibility of a triple cascade. Since the balance seems to be quite low energy, the impression of small competition given by the curve is especially misleading. To illustrate, suppose we assume rashly that the 20% of the counts (extrapolated to true zero absorber) are due to competition of a branch comprising three equal γ's in cascade. Then 3/4 of the radiation quanta are of this sort, and 1/4 the full energy, which implies equal branching.

That the discrepancy at thin absorbers is not simply a result of using

---

* The use of the curves on tracing paper facilitates this operation.

inappropriate "master" curves is shown by Figures (10) and (11), where the radiation from the 0.55 and 1.76 Mev resonances is very well fitted by the assumption of pure ground state transitions.

The radiation from the 2.10 Mev resonance does not exhibit 9 Mev quanta at all, and this time the graphical analysis indicates a cascade process by 6 and 3 Mev steps.

The other weak resonance, at 1.16 Mev exhibits a mixed radiation also, but its analysis is further complicated by its location astride the broad 1.3 Mev resonance. The same target was used as for the excitation function shown in Figure 6. Subtraction of 30% of the absorption function obtained at 1.3 Mev from that obtained at 1.16 Mev does not eliminate the 8.6 Mev tail, but reduces its contribution (at true zero) from 35% to 25% (in counting rate) and makes the balance resemble 2.5 Mev rather than 3 Mev.

We may conclude that

(a) the strong resonances at 0.55 and 1.76 Mev radiate primarily to the ground state;

(b) the broad resonance does so only about half the time, the balance being by low energy cascade;

(c) the 2.10 Mev resonance decays by a cascade involving γ's of about 6 and 3 Mev;

(d) the radiation at 1.16 Mev cannot be disentangled by the present analysis.

The absorption curves are summarized in Figure 12.

Considerable interest has been aroused by this complex spectrum, but its low intensity makes spectrometer techniques difficult to apply. Preliminary examination of the stronger resonances with NaI scintillation crystals[24] indicated much more sensitive detection of the softer components. More information on the spectrum should be forthcoming.

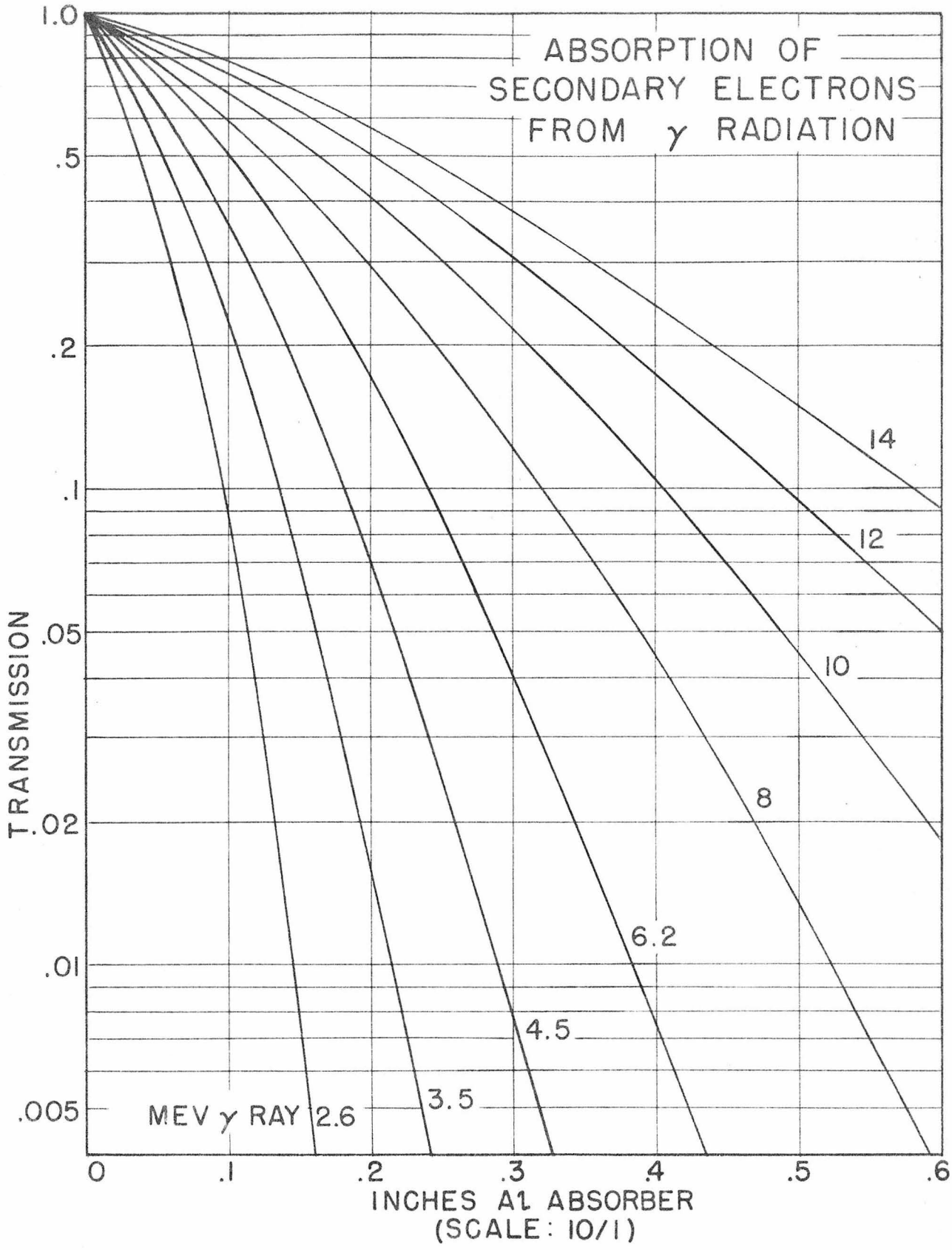
ABSORPTION OF
SECONDARY ELECTRONS
FROM γ RADIATION
1.0
.5
.2
.1
.05
.02
.01
.005
TRANSMISSION
14
12
10
8
6.2
4.5
3.5
2.6
MEV γ RAY
0
.1
.2
.3
.4
.5
.6
INCHES Al ABSORBER
(SCALE: 10/1)

FIG. 8

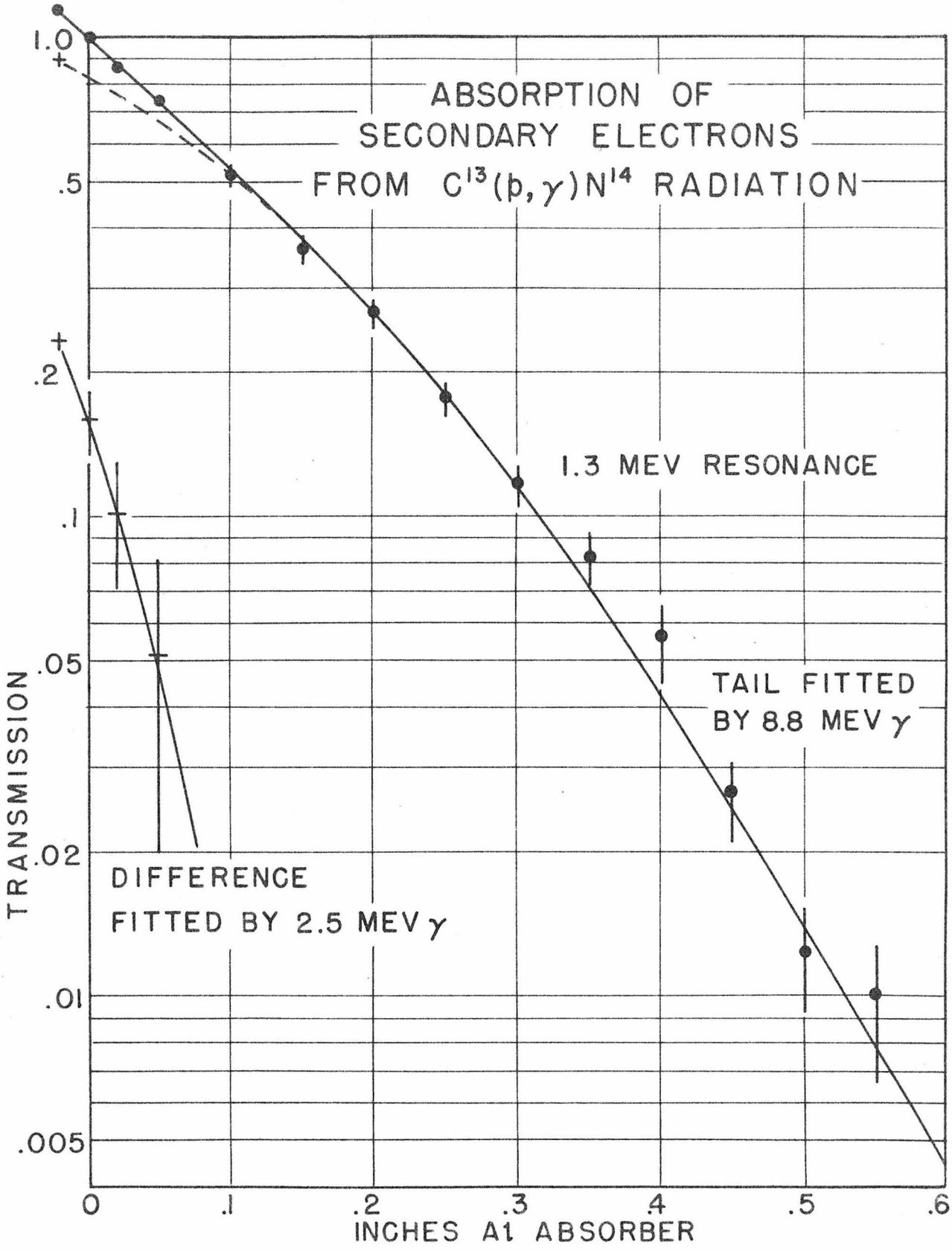
ABSORPTION OF
SECONDARY ELECTRONS
FROM $C^{13}(p,\gamma)N^{14}$ RADIATION
1.3 MEV RESONANCE
TAIL FITTED
BY 8.8 MEV γ
DIFFERENCE
FITTED BY 2.5 MEV γ
TRANSMISSION
1.0
.5
.2
.1
.05
.02
.01
.005
0
.1
.2
.3
.4
.5
.6
INCHES Al ABSORBER

FIG. 9

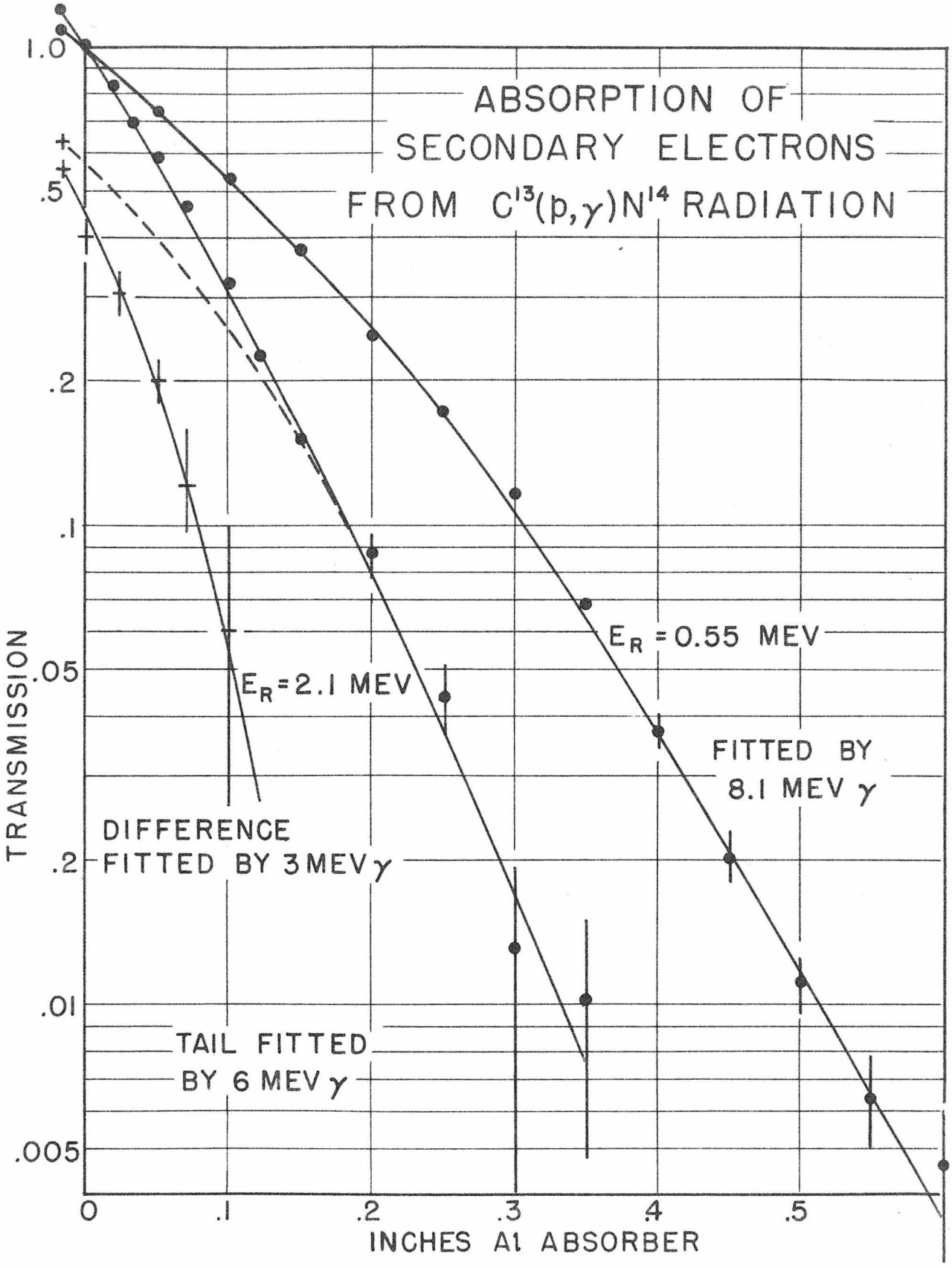
ABSORPTION OF
SECONDARY ELECTRONS
FROM $C^{13}(p,\gamma)N^{14}$ RADIATION
TRANSMISSION
1.0
.5
.2
.1
.05
.2
.01
.005
E_R = 0.55 MEV
FITTED BY
8.1 MEV γ
E_R = 2.1 MEV
DIFFERENCE
FITTED BY 3 MEV γ
TAIL FITTED
BY 6 MEV γ
0
.1
.2
.3
.4
.5
INCHES Al ABSORBER

FIG. 10

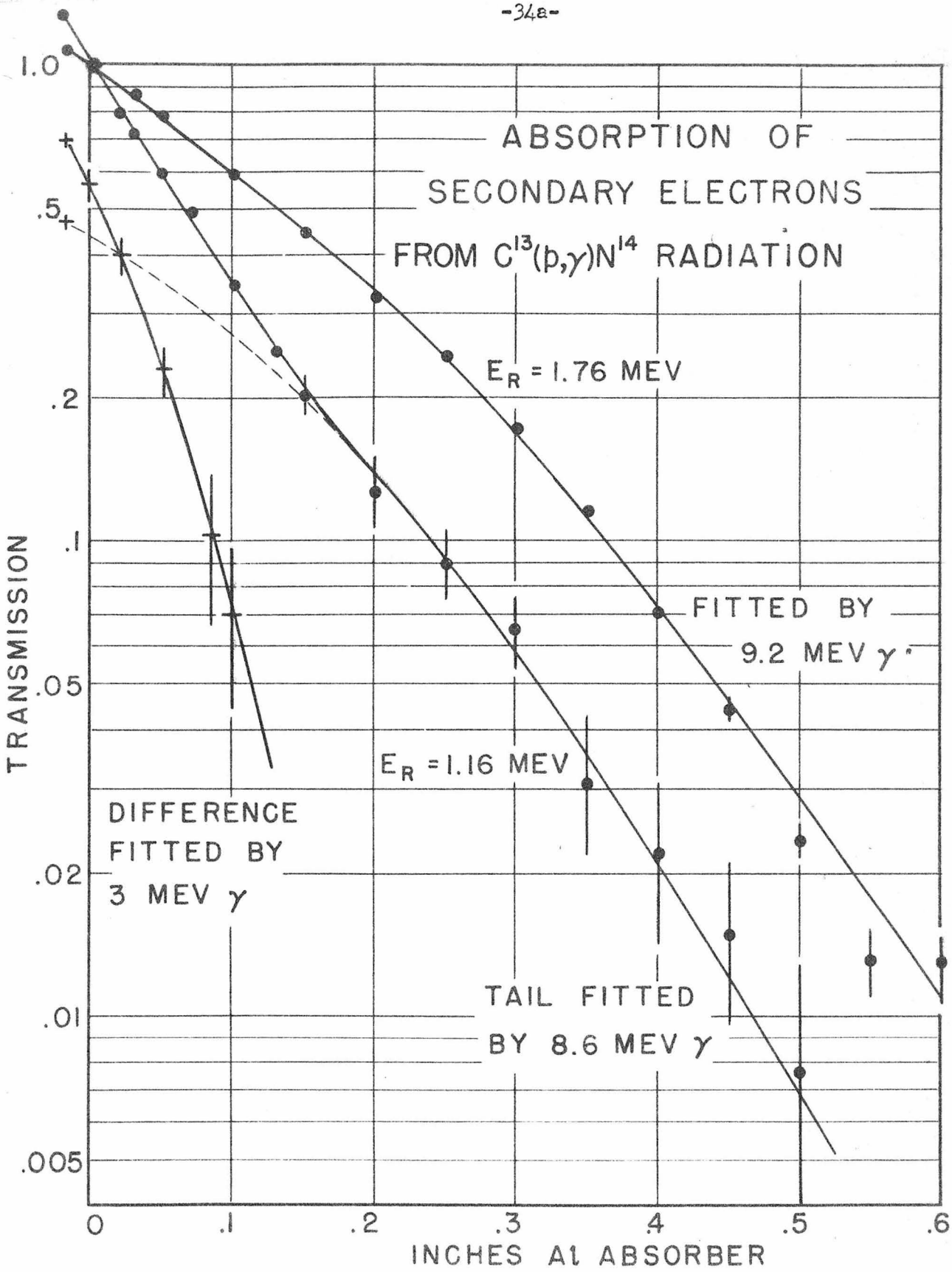
ABSORPTION OF
SECONDARY ELECTRONS
FROM $C^{13}(p,\gamma)N^{14}$ RADIATION
E_R = 1.76 MEV
FITTED BY
9.2 MEV γ
E_R = 1.16 MEV
DIFFERENCE
FITTED BY
3 MEV γ
TAIL FITTED
BY 8.6 MEV γ
TRANSMISSION
1.0
.5
.2
.1
.05
.02
.01
.005
0
.1
.2
.3
.4
.5
.6
INCHES Al ABSORBER

FIG. 11

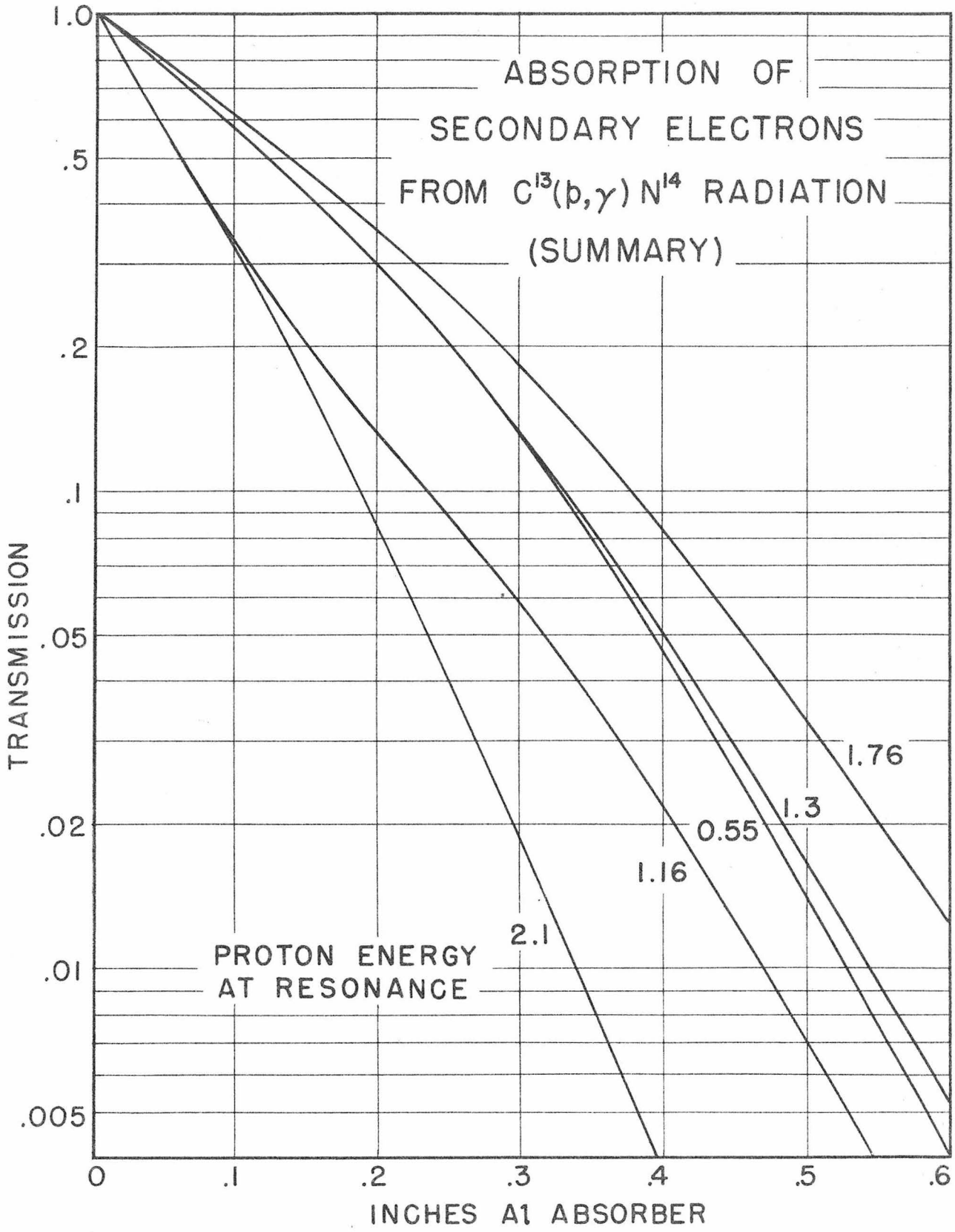
ABSORPTION OF
SECONDARY ELECTRONS
FROM C13(p,γ) N14 RADIATION
(SUMMARY)
TRANSMISSION
1.0
.5
.2
.1
.05
.02
.01
.005
0
.1
.2
.3
.4
.5
.6
INCHES Al ABSORBER
1.76
1.3
0.55
1.16
2.1
PROTON ENERGY
AT RESONANCE

FIG. 12

VI. THE ABSOLUTE YIELDS

Although results obtained in relative excitation functions and comparisons made with a given experimental set-up can be considered as reasonably secure, and in many cases relative intensities can be measured to high precision, the measurement and calculation of absolute intensities, or the comparison of radiation differing greatly in intensity or composition encounters serious experimental limitations, some of which will be discussed below.

Because of the dependence of cross-sections and radiation widths on absolute yields, and the interest in the part played by the carbon (p,γ) reactions in the "carbon cycle" of energy production, the problem of the absolute yields has been approached in several different ways, involving:

(a) direct calculation of detection efficiency;

(b) comparison with the well known thick target yield from fluorine;

(c) comparison of the yields due to C^{12} and C^{13} from a thick target of normal graphite; and

(d) an independent determination of the $C^{12}(p,\gamma)N^{13}$ yield from the concomitant yield of $N^{13}(\beta^+)C^{13}$.

The following considerations have been taken into account in making absolute measurements and comparisons:

1. The detection efficiency. Equation (16) for "aluminum walls" may be used as the maximum efficiency approached by using a converter just thicker than the maximum range of the secondary electrons produced by the radiation in question. The counter tube was surrounded by a set of nesting cylindrical sleeves totaling 1.51 cm in thickness, which is sufficiently thick to give saturation intensity of secondaries from 8 Mev radiation, and also to stop the pairs accompanying the 6.3 Mev radiation from fluorine. (see paragraph 4.)

2. The effective solid angle of radiation intercepted, which is somewhat less than (area)/(distance)^2, since the ends of the sensitive volume are farther from a symmetrically placed source than is the center, and the actual counting volume is cylindrical, and secondaries are scattered into it from all directions. These geometrical factors are discussed in detail in Reference (19), P. 269. The corrections mentioned amount to 7% for the counter used, at a distance of 10.0 cm from the target spot. Measurement of the sensitive area is subject to an uncertainty of 5%.

3. The attenuation of the primary radiation in the aluminum converter (7.8% for 6.3 Mev radiation), and in the brass walls of the target chamber (2.6%).

4. In the case of fluorine, about 1/2% of the yield at 1 Mev is in the form of nuclear pairs, which could give rise to as much as 10% excess counting rate, were they not stopped in the converter. Detection of annihilation radiation from the positrons is negligible.

5. Angular distributions. The radiation from the low resonances in C^{12} and C^{13} are known to be essentially isotropic[11], and the thick target yield from fluorine very nearly so. What has actually been measured is 4π times the differential yield at 90^{o}. The thick target yield measured in this manner has been given as 6.9×10^{-7} disintegrations/proton at 960 kev by Fowler and Lauritsen[5], and found to be 3% greater at 1.000 Mev*, which is consistent with the value of 7.1×10^{-7} obtained from the more recent results of Chao, et. al[25] taking into account the small anisotropy of radiation.

6. Counting rate loss due to the dead time of the counters and associated equipment. The dead time and recovery time were found with the aid of a synchroscope to be about 250 microseconds each. Since these were

---

* R. B. Day and E. J. Woodbury, private communications.

surprisingly low, the counting rate loss for the entire counter-scalar-register system was checked by varying the proton current on a fluorine target, and the effective loss found empirically to be 1% at 250 counts per second. Counting rates were kept well below this value.

7. Current and charge measurement. The leakage rate from the current-integrating condenser was measured, and was found to be a source of not more than 0.1% error. The absolute value of the condensers was known to 1%. The integrator trigger circuit was set to stop the counters when the condenser had charged up to 50.0 volts. The target tube itself formed a deep Faraday cage for charge collection, and a guard ring held at − 300 volts with respect to ground was used to suppress any secondary electrons. Two sets of tantalum trimming slits and an additional diaphragm insured that no charge was being collected which did not strike the target. The CaF_2 crystal used as a fluorine target was crossed with fine tungsten wires just outside the area bombarded to minimize the tendency to charge up and spark to the target support.

8. The C^{13} target was the same one used for the excitation functions and absorption curves, and for which $Y = 0.50\ Y_{max}$ as discussed in connection with the measurement of the width of the lowest resonance. A local excitation curve was run to be certain no layer of contamination had shifted the peak. Mass Two (H_2^+) was used, but as discussed in connection with the excitation function any thin target yield from normal deuteron contamination should be quite negligible. In the calculations due account has been taken that each microampere of H_2^+ corresponds to <u>two</u> microamperes of protons.

9. Since the intensities as <u>measured</u> (counts/μ coul) for F and C^{13} differed by a factor of 111, and the background was about 0.3% of the maximum allowable counting rate, and moreover the accelerator would not operate and regulate properly for a beam-current range much exceeding a factor of a few hundred, it was necessary to place the counter at a distance from the target

so chosen that at the minimum beam current the fluorine counting rate was reasonable, and yet that from C^{13} at the maximum beam was well above the background, in addition to satisfying the requirement that the geometrical correction discussed under (2) be small. A distance of 10 cm was chosen from preliminary estimates of the yields and operating conditions.

10. To attenuate the large background counting rate, the counter and target tube were completely surrounded by a large box of lead bricks 2" thick, lined with 3/8" aluminum to minimize scattering-in of radiation. A A smaller counter placed closer to the source would have shown a proportionately smaller background, but it was thought desirable to use the same Geiger tube used previously as the front counter in the coincidence experiments. The background values were obtained with the beam striking a clean tantalum surface mounted on the back of the rotatable target support, so as to include possible effects of radiation from the defining slits or X-rays from the tantalum backing. In the case of the C^{13} target, the background from the accelerator amounted to some 7% of the counts, and to allow for any irregular variation, runs lasting about a minute were taken alternately on target and on background, and a small time-dependent correction made. Both the raw data and net values exhibited normal statistical fluctuations, and enough cycles were taken to insure results statistically significant to 1%.

A yield of 1940 counts/microcoulomb was found for fluorine at 1 Mev. Using as the effective solid angle 1.62% of a sphere, the absorption corrections mentioned above, the ratio 6.24×10^{12} protons/microcoulomb, and an efficiency of 0.70 (6.3 Mev) = 4.41%*, the yield calculated is 6.90×10^{-7} γ/p. This agrees with the expected yield to well within the uncertainties of the calculations. If we adopt 7.1 as the standard value, other measurements may

---

* The actual thick target yield is a complicated mixture of 6.14, 6.91, and 7.11 Mev radiation, but if the intensities in Table V of Reference (25) are weighted according to their respective energies, the effective energy is 6.3 Mev.

be corrected in the ratio 7.1/6.9.

The corresponding result for C^{13} was 8.70 counts/microcoulomb (of protons). By a similar calculation, including the additional factor of 2.0 to correct the thin to thick target yield, and the 3.6% correction from the fluorine standardization, we find a yield of 4.9×10^{-9} for the target taken to be 61% C^{13}. The yield for pure C^{13} would then be 8.0×10^{-9}, and 0.9×10^{-10} for a normal (1.12%) carbon target.

This is in agreement with previous comparisons made with somewhat larger uncertainties. It must be recognized in quoting "absolute" figures, and applying small "corrections", that it is very difficult to validate the calculation of absolute yields to much better than 10%. The value used for the fluorine yield may not be very much more precise.

VII. COMPARISON OF C^{12} AND C^{13} YIELDS IN NORMAL CARBON

Before enriched material was available, the thick target yield from C^{13} was estimated from the excitation function by an attempt to disentangle the "double step". This is a very difficult experiment. The yield is of the order of $10^{-9} \gamma/p$, or $6 \times 10^{3} \gamma/\mu$ coul. In order to calculate the effective solid angle, and minimize uncertainties in the calculation due to differences in the distribution of the secondaries from 2.4 and 8 Mev radiation, it was necessary to place the counter so as to intercept only about 2% of the radiation, which moreover was detected with an efficiency of less than 2% (for C^{12}), so that the counting rate is only a few counts/sec with as much as a microampere of protons. This makes collection of statistically significant information extremely tedious and insecure. In addition, the annihilation radiation from N^{13} positron activity built up during long bombardments contributes a noticeable part of the counts recorded. With the aid of coincidence counting of the high energy radiation and positron counting of

the N^{13} yield, Fowler and Lauritsen* were able to study the shapes of the two excitation functions in the vicinity of 0.5 Mev. They were found to be somewhat unsymmetrical about the half-maximum point, and the widths reported were the energy differences between the 3/4 and 1/4 maximum points. Both yield functions were found to continue to rise well "beyond" the resonances. The yields reported were 7.2×10^{-10} for C^{12} and 1.8×10^{-10} for C^{13}. The latter is twice that calculated above for the most reliable enriched target data. This discrepancy was noted in earlier preliminary calculations, and an investigation of possible contamination in the thin target pursued. The thin targets exonerated**, it was thought of interest to try to repeat the above experiment on the 3 Mev accelerator.

This was done with a similar counter at the same distance from the target (8 cm) used by Fowler, enclosed in the aluminum-lined lead house described above. By the use of the copious H_2^+ component of the beam, equivalent to 4 microamperes of protons, it was possible to obtain data with a 3% statistical error in a bombardment lasting only 2 minutes. In addition to the greater statistical accuracy attainable with the much higher counting rate, it is felt that in this case the contribution of the annihilation radiation was nearly all included in the background measurements, which were made between every few points (during a 2 minute count the average counting rate due to a 10 minute half-life decay is only 7% less than the rate at the beginning of the counting period.). The results are shown in Figure 13. The double excitation function was analyzed with the use of Fowler's positron excitation curve, and the thick target γ curve obtained with enriched material. The positron data, normalized in amplitude to agree at the point of inflection, is in complete agreement with our γ yield. The enriched target curve, whose shape is now well established, was adjusted in

---

* This data is presented in Figure 1 of Reference (19), P. 243.

** 1/2% of iodine would increase the stopping cross-section by only 2%.

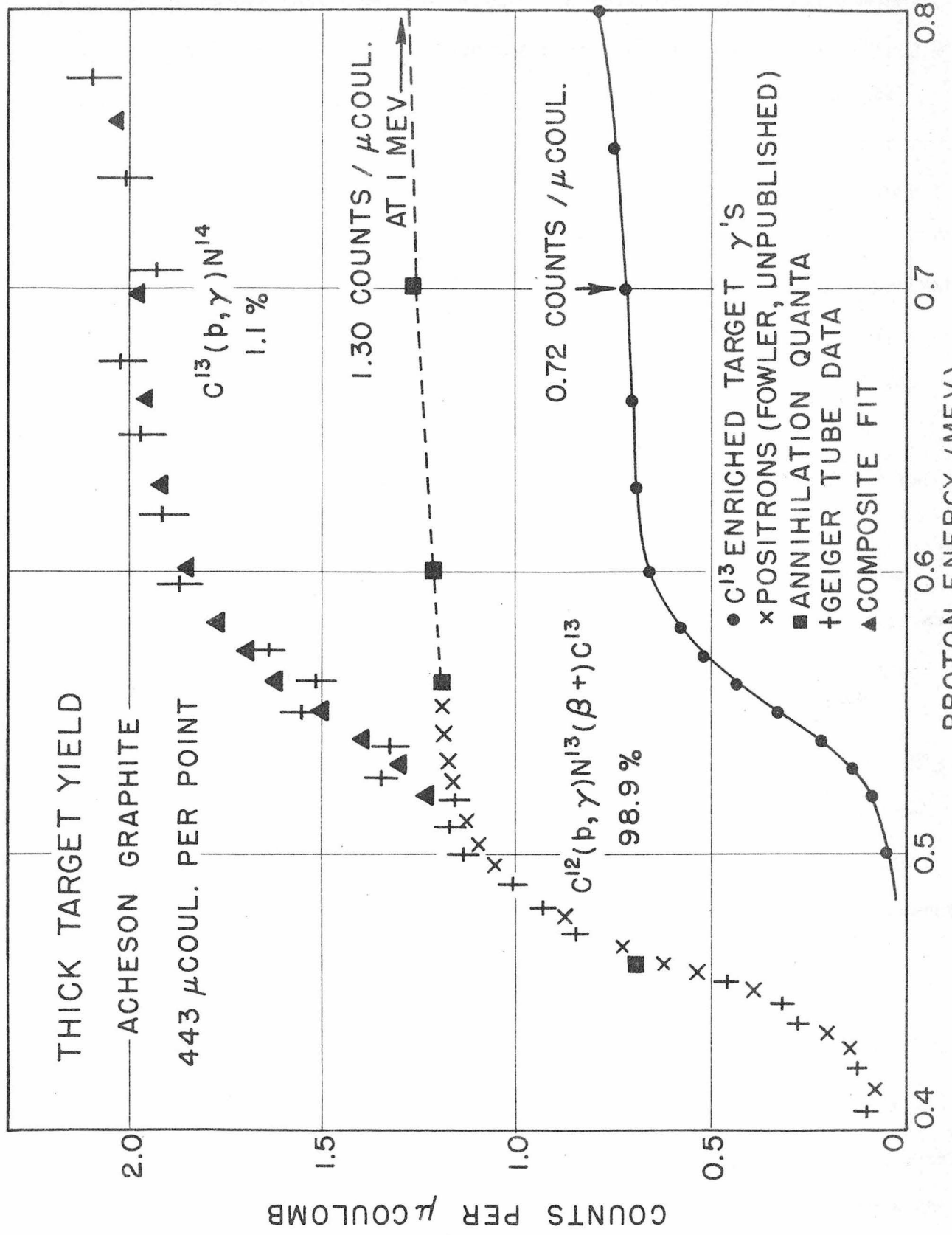
THICK TARGET YIELD
ACHESON GRAPHITE
443 μCOUL. PER POINT
C13(b,γ)N14
1.1 %
1.30 COUNTS / μCOUL.
AT 1 MEV
0.72 COUNTS / μCOUL.
C12(b,γ)N13(β+)C13
98.9 %
● C13 ENRICHED TARGET γ'S
× POSITRONS (FOWLER, UNPUBLISHED)
■ ANNIHILATION QUANTA
+ GEIGER TUBE DATA
▲ COMPOSITE FIT
COUNTS PER μCOULOMB
PROTON ENERGY (MEV)
0
0.5
1.0
1.5
2.0
0.4
0.5
0.6
0.7
0.8

FIG. 13

amplitude to secure best agreement with the normal yield curve when added to the positron curve. The points on the positron curve marked "Annihilation Quanta" are from an entirely different experiment to be described in the next section. In view of the serious statistical scatter of the earlier γ data (not shown), it is in (rough) agreement with the excitation function shown here, both as to shape and observed counting rate.

However, detailed interpretation of the curve in the manner shown (with the advantage of hindsight about the separate shapes) gives considerably different results. Fluorine at 1 Mev was used as a check, and a value of $6.9 \times 10^{-7} \gamma/p$ calculated from an independent set of geometrical values. Using the above analysis, the yields calculated are 7.0×10^{-10} for C^{12} (at 1 Mev) and 1.1×10^{-10} for C^{13} (at 700 kev).

At the time this experiment was performed only 0.87 cm of aluminum converter was employed. From a curve showing the building-up of secondaries from 7.4 Mev $Be^9(p,\gamma)$ radiation to within 4% of saturation for this thickness, the loss for 6.3 and 8.1 Mev radiation can be estimated from our absorption curves as 2% and 5%, respectively. In the case of fluorine, this loss would be made up by about 2% excess counts from the pairs. This correction would raise the C^{13} figure to $1.15 \pm 0.15 \times 10^{-10}$. We will return to the question of the C^{13} yield after discussing the independent measurement of the C^{12} yield mentioned above.

VIII. THE THICK TARGET YIELD OF $C^{12}(p,\gamma)N^{13}$

Advantage was taken of the scintillation counter and associated equipment used by Walker and Day[24] to obtain the thick target excitation function of $C^{12}(p,\gamma)N^{13}$ from the $N^{13}(\beta^+)C^{13}$ activity produced in the targets. Difficulties attending absolute beta detection were circumvented by removing the targets from the vacuum system and placing them in a standard position on the light shield directly over the NaI crystal and photomultiplier. The

targets were covered by a recessed block of aluminum, so the positrons were annihilated in the immediate vicinity of the targets. The targets were pills turned (dry) from a block of Acheson graphite. They were held by the edge in a recess in a quick-change target probe, and clamped firmly in place from the rear by a phosphor bronze spring strap. The target could be rotated to one side and the beam accurately aligned on a quartz window. Loss of N^{13} by diffusion out of the graphite was considered to be negligible at the moderate temperatures developed in the targets, as no build-up of activity was detected by a shielded Geiger counter placed in the exhaust line of the target system pumping system.

N^{13} has a half-life of 10.1 minutes[26], and a corresponding decay constant $\lambda = 1.142 \times 10^{-3}$ sec^{-1}. If the target is bombarded for a time t_b with a proton current i, allowed to decay for a time t_d, and then counted for a time t_c by a counter whose effective efficiency is $f = 2 \epsilon_{.51} \Omega$, then

$$\text{Counts recorded} = \text{Yield} \times f \times i \lambda^{-1} \underbrace{(1 - e^{-\lambda t_b})}_{\text{bombardment}} \; e^{-\lambda t_d} \; \underbrace{(1 - e^{-\lambda t_c})}_{\text{counting}} \qquad (18)$$

For $\lambda t_b << 1$, the bombardment factor can be expanded in a rapidly convergent series, and (it_b) set equal to the total charge q collected by the integrator, so that the bombardment factor in Equation (18) is

$$q \left[1 - (\lambda t_b)/2 + (\lambda t_b)^2/6 + \ldots\right]. \qquad (19)$$

The effect of rapid current variations was smoothed out, and since t_b did not exceed a few minutes, the approximation made in obtaining (19) was negligible. For an example of the quantities involved, bombarding at 1 Mev, collecting 222 microcoulombs in 200 seconds, followed by a delay of 90 seconds, and counting for 240 seconds led to about 15 kilocounts, about 1/5 of the ultimate, and giving less than 1% random counting error.

The excitation function for the reaction was taken between 0.45 and 2.2 Mev with (a) a single channel differential pulse analyzer straddling the

annihilation photo-peak, and simultaneously with (b) a discriminator set just below the peak. Because of drifts in the differential channel setting, the differential data showed somewhat larger scatter than the integral data, which reproduced within the expected random error. The integral data, corrected to ultimate values by Equation (18), is shown in Figure 14, and is believed to give the relative excitation function to $\pm$ 1%. The upper resonance is located at 1.70 $\pm$ .008 Mev, and has a width of 70 $\pm$ 5 kev. The curve corresponds to the integral of a symmetrical Breit-Wigner resonance. The ratio of yields at 2.00 and 1.00 Mev is found to be 2.39 $\pm$ .05. The yield at 2.00 Mev from a 70 kev resonance at 1.70 Mev is expected to be 4.5% short of $Y_{max}(\infty)$, so from our data we may conclude that the total yield of the upper resonance is 1.45 $\pm$ .03 times that of the lower resonance, a result which is in agreement with, but more precise than the value 1.3 $\pm$ .2 given by Van Patter[7].

The effective efficiency f was determined by comparison of the counting rate in the annihilation channel with the strength of a Na^{22} source placed in the standard position. The source strength was compared on a Geiger-tube "bench" with that of a "standard" Na^{22} source determined by T. Lauritsen in a β-spectrometer as 3.53×10^6 disintegrations/sec ($\pm$ 5%) on 27 February, 1951. This value itself was determined by comparison of the 1.2 Mev γ line with a standard Co^{60} source. Allowing for a 3% decay (2.6 yr half-life) since the time of determination, the weak source prepared was found to have a source strength of 3.0×10^4 disintegrations/sec ($\pm$ 5.5%). This gave the efficiency as 5.0%. Finally, two separate comparisons of the radiation in the annihilation channel from N^{13} at E_p = 1.00 Mev and that from the Na^{22} source were made, and allowing for a systematic error of about 10% due to radiation scattered into the annihilation channel from the 1.2 Mev line (determined from the complete integral and differential bias curves), the yield of $C^{12}(p,\gamma)N^{13}$ was

determined as 7.7×10^{-10} N^{13}/proton for normal carbon at $E_p = 1.00$ Mev, which is in agreement with the value previously reported[5], 7.3×10^{-10} ($\pm$ 10%). Averaging these two independent determinations, we may conclude that the yield is 7.5×10^{-10} N^{13}/proton ($\pm$ 7%).

A further check on the ratio of C^{12} to C^{13} yields at 0.5 Mev may be obtained from the ratios at 1.7 Mev in a somewhat circuitous manner indicated by the identity

$$\left(\frac{C^{12}_{0.45}}{C^{13}_{0.55}}\right) = \left(\frac{C^{13}_{1.76}}{C^{13}_{0.55}}\right)\left(\frac{C^{12}_{1.70}}{C^{13}_{1.76}}\right)\left(\frac{C^{12}_{0.45}}{C^{12}_{1.70}}\right) \quad . \qquad (20)$$

The first ratio on the right is 1.47 (at 90°) from the enriched thick target yield (Table I), and the third ratio was determined in the experiment just described, namely 1/(1.45). The C^{12}/C^{13} ratio at 1.7 Mev is the limiting factor both in magnitude in precision, the others being known to a few percent.

In some respects, this ratio is harder to obtain than that at 0.5 Mev, since the yields are still small and both thick target "steps" must be subtracted from the total yield, magnifying statistical uncertainties. Moreover, both upper resonances have a marked angular distribution[13].

From the thick target data, Day estimates the upper ratio of coincidence counts at 90° as 2.8 $\pm$ 0.3. By a numerical integration of the two components of a thin target excitation curve, a corresponding value of 2.4 $\pm$ 0.3 was obtained (by use of Equation (15), the target thickness cancels out in the ratio). Using the average value of these determinations, and allowing for the absorption in the converter and absorber, the counter efficiency, and the angular distribution in the case of C^{12}(that of C^{13} cancels out), the ratio of yields should be 8.8 $\pm$ 1 at 1.7 Mev and 9.0 $\pm$ 1.5 at 0.5 Mev. If the C^{12} yield is 7.5×10^{-10}, that of C^{13} is predicted by this method to be 0.83 $\pm$ $.15 \times 10^{-10}$. This check confirms the determination of the yield found with the enriched thin target, but does not contribute any additional precision.

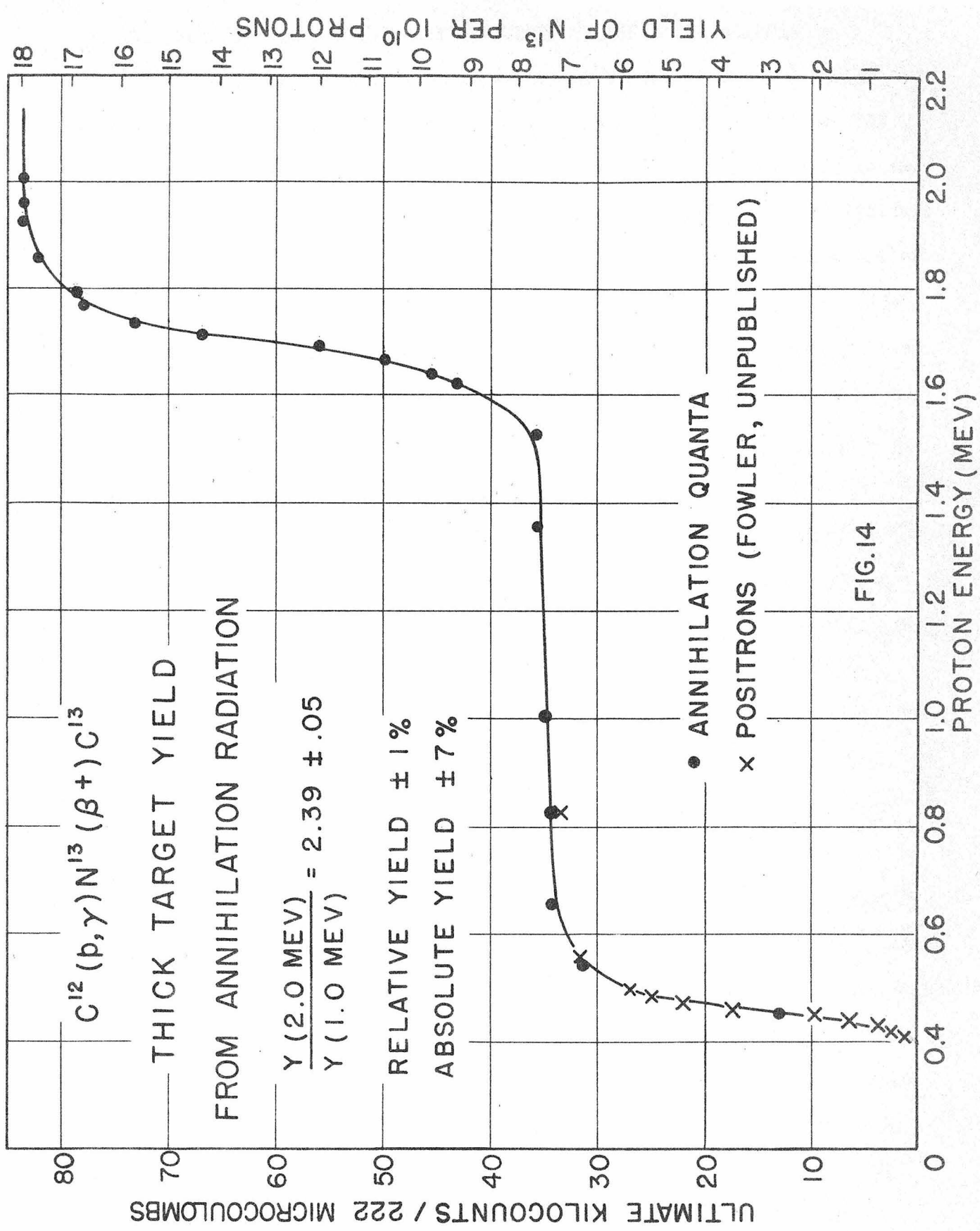
$C^{12}(b,\gamma)N^{13}(\beta+)C^{13}$
THICK TARGET YIELD
FROM ANNIHILATION RADIATION
$\frac{Y(2.0\ MEV)}{Y(1.0\ MEV)} = 2.39 \pm .05$
RELATIVE YIELD ±1%
ABSOLUTE YIELD ±7%
• ANNIHILATION QUANTA
× POSITRONS (FOWLER, UNPUBLISHED)
ULTIMATE KILOCOUNTS / 222 MICROCOULOMBS
YIELD OF N^{13} PER 10^{10} PROTONS
PROTON ENERGY (MEV)
0
0.4
0.6
0.8
1.0
1.2
1.4
1.6
1.8
2.0
2.2
10
20
30
40
50
60
70
80
1
2
3
4
5
6
7
8
9
10
11
12
13
14
15
16
17
18

FIG.14

IX. SCINTILLATION COUNTER MEASUREMENTS OF THE N^{14} RADIATION

E. J. Woodbury at this laboratory has used some of the C^{13} enriched targets in an investigation[29] of the yield of the (p,γ) reaction at 130 kev in connection with the extrapolation to 30 kev, the proton energy in the interior of the sun most effective for this process. For this very difficult measurement he has developed an ingenious electronic system, and made use of the scintillation pulses produced in a NaI crystal by γ radiation. In addition to the advantage of greater efficiency for detecting γ radiation than is found in Geiger counters, the distribution of pulse sizes detected by the photomultiplier is related in a characteristic way to the γ energy. For his geometry, he found that the integral bias curve (number of pulses above a given size as a function of size) for a single energy was very nearly linear (almost uniform distribution), so that mixtures can be analyzed graphically in much the same manner as the Geiger coincidence absorption measurements, but on a linear scale. Also, the detection efficiency (proportional to the absorption coefficient for NaI) is very nearly independent of energy between 2 and 10 Mev, which is a great advantage over the Geiger tube method for detecting low energy quanta in the presence of others of high energy. In the experiment at low energy (and extremely low yield), it was desirable to use as high a bias as possible to cut down background, and therefore necessary for him to know how the N^{14} spectrum appeared in his apparatus, at least for the 0.55 and 1.25 Mev resonances. The latter, because of its great width, contributes appreciably to the yield at very low energies.

Measurements were made with this apparatus on the 3 Mev accelerator, at all five resonances, and gave information to supplement the absorption curves. Details are given in Woodbury's thesis[29], and only the general results will be given here, in Table IV:

TABLE IV

E_R	Character of the Spectrum (γ's)
0.55 Mev	70% 8 Mev, 30% ~2 1/2 Mev
1.16	40% ~4 Mev, 60% ~2 1/2 Mev
1.25	75% 8 Mev, 15% ~3 1/2 Mev, 10% <1 Mev
1.76	85% 9 Mev, 15% ~2 1/2 Mev
2.10	all 4 or 5 Mev.

Table IV gives the composition of the N^{14} radiation as determined graphically from the integral bias curves. The fractions and energies indicated are subject to the same uncertainties as were involved in interpretation of the absorption curves, but with the important difference that here the soft components are resolved as sensitively as the hard. The results are consistent with the Geiger tube results which were (linearly) weighted in favor of the hard component. It is not yet possible to make definite assignments of levels and transitions, beyond the strong suggestion that the "2 1/2" Mev line is the transition to the ground state from the well-known first excited level at 2.3 Mev. A very low energy contribution appears only in the broad resonance.

The scintillation counter was calibrated with the thick target yield of fluorine at 1 Mev, and assuming the detection efficiency varies with the absorption coefficient, Woodbury calculates for the yield of the 0.55 Mev resonance of C^{13} in normal carbon: 0.9×10^{-10} dis./proton for the hard component, and a total of 1.0×10^{-10} dis./proton if the soft components are interpreted as three equal γ's in cascade. This determination is also subject to a (systematic) uncertainty of $\pm$ 10%, and is in agreement with the yields found previously.

It is also clear that more precise determination of the absolute yields awaits more precise knowledge of the spectrum. The theorem mentioned on P. 19 that Geiger tubes measure disintegrations, independent of branching and cascades, is not quite valid if the energies are very different and unknown, since softer components are more attenuated in the thick converter necessary for the hard component.

Taking into account all the approaches to the absolute yield discussed, we may conclude for the time being that the yield of the 0.55 Mev resonance in $C^{13}(p,\gamma)N^{14}$ is 1.0×10^{-10} dis./proton in normal carbon, or 9.0×10^{-9} dis./proton in pure C^{13}. These values must be regarded as subject to an uncertainty of about 10% in excess of that on the fluorine yield.

R. W. Walker and R. B. Day have recently reported[24] on an application of differential scintillation spectroscopy to this and other problems. They find a 2.3 Mev γ present at the 0.55 Mev resonance, but a 5.8 Mev γ line is definitely absent. There is a suggestion of much weaker 4 Mev radiation (possibly from the broad resonance). It is hoped that their promising technique will shortly be brought to bear in more detail on this and the other resonances, as it offers a most encouraging hope of disentangling this complicated spectrum. It is also hoped to examine the more intense radiation with a β-spectrometer.

X. WIDTHS AND CROSS-SECTIONS

More information about the reaction can be obtained from the measurements by examining more closely the structure of the cross-section formula. The complete single-level Breit-Wigner dispersion formula[27] for a (p,γ) process may be written

$$\sigma = \pi \lambda^2 \frac{\omega \Gamma_\gamma \Gamma_p}{(E - E_R)^2 + \Gamma^2/4} \qquad (21)$$

where $2\pi\lambda\!\!\!^{-}$ is the de Broglie wave length of the incident proton (in the center-of-mass system), Γ_p is the width for re-emission of the proton from the compound nucleus, Γ_γ is the width for radiation*, $\Gamma = \Gamma_\gamma + \Gamma_p \simeq \Gamma_p$ since $\Gamma_\gamma << \Gamma_p$, and ω is a statistical factor involving the spin i of the incident particle (1/2 for proton), the total angular momentum (or "spin") I of the target nucleus (0 for C^{12}, 1/2 for C^{13}), and the total angular momentum J of the compound state:

$$\omega = \frac{2J+1}{(2i+1)(2I+1)} = (2J+1) \begin{cases} 1/2 \text{ for } C^{12} \\ 1/4 \text{ for } C^{13} \end{cases} \tag{22}$$

Setting $\Gamma_p = \Gamma$ in Equation (21), we find that

$$\sigma_R = 4\pi\lambda\!\!\!^{-}_R{}^2 \frac{\omega\Gamma_\gamma}{\Gamma}, \tag{23}$$

so that from Equation (13), the maximum thick target yield

$$Y_{max}(\infty) = \frac{2\pi^2\lambda\!\!\!^{-}{}^2\omega\Gamma_\gamma}{\varepsilon_d}, \tag{24}$$

and is independent of the proton width. Noting that $\lambda\!\!\!^{-}{}^2$ is inversely proportional to the bombarding energy, we could compute relative values of $\omega\Gamma_\gamma$ without reference to the absolute yields. Numerically, however,

$$2\pi^2\lambda\!\!\!^{-}{}^2 = \frac{1}{2}\left(\frac{h^2}{2ME}\right) = \frac{1}{4}\left(\frac{h}{Mc}\right)^2\left(\frac{M}{m}\right)\left(\frac{mc^2}{E}\right) = \frac{4.74 \text{ barns}}{E_{lab}, \text{ in Mev}}, \tag{25}$$

where $h/Mc = 1.32 \times 10^{-13}$ cm is the "Compton wave length" of the proton, $mc^2 = 0.51$ Mev, the rest energy of the electron, $M/m = 1837$, and one "barn" $= 10^{-24}$ cm^2. $E_{c.m.}$ has been converted to E_{lab} by the factor $(13/14)^2$. The numerical factor in Equation (25) would be 4.79 for C^{12}. The cross-sections encountered here will be on the order of a millibarn (1 mb $= 10^{-27}$ cm^2), which can be anticipated by writing Equation (23) as

$$\sigma_R = 0.301\left(\frac{1 \text{ Mev}}{E_R}\right)\left(\frac{\omega\Gamma_\gamma}{1 \text{ ev}}\right)\left(\frac{10 \text{ kev}}{\Gamma}\right) \text{ millibarns.} \tag{26}$$

---

* In the case of cascade radiation, Γ_γ is the width for the first stage.

The proton width Γ_p, which is a measure of the rate of decay of the compound nucleus by proton emission depends on

(a) The probability of penetrating the Coulomb barrier (the Gamow factor),

(b) The proton velocity, or rate of encountering the barrier, and

(c) Specifically nuclear properties, selection rules, etc.

If the angular momentum L of the incoming protons is known, factor (a) can be calculated, and an estimate of the essentially nuclear width obtained. For this purpose it is convenient to so normalize this "width factor" to include the velocity dependence. Christy[28] has calculated these factors for the light nuclei in such a manner as to give the nuclear "width without barrier" G for a proton of 1 Mev energy. The results for carbon are reproduced in Figure (15), in which are plotted the "width factors" $E^{1/2} \cdot P_L$ for E in Mev as a function of $E^{-1/2}$, the scale being chosen so that at low energy the curves approach straight lines.

Also shown in Figure (15) is the stopping cross-section for carbon, and a quantity $(\varepsilon E^{1/2})/P_0$, which was conveniently calculated graphically. The use of this quantity is illustrated in Figure (16), where it is shown plotted on a linear energy scale, together with the smoothed thin target yield for the 1.3 Mev resonance. Since for this very broad resonance, none of the quantities λ, ε, or Γ which appear in the yield integral of Equation (9) are constants, the observed curve is noticeably unsymmetrical. But since they appear in the combination $(\lambda^2 \varepsilon / \Gamma)$ multiplying the resonance denominator term, the curve should be reducible to a function showing only the latter term by multiplying the yield curve by the inverse of the former term, or by what is more convenient, $(\varepsilon E^{1/2})/P_0$. This "reduced" curve is also shown, and does appear much more nearly symmetrical, with its peak shifted down to 1.25 Mev, and with a half-width of 500 kev. Of course, the Γ

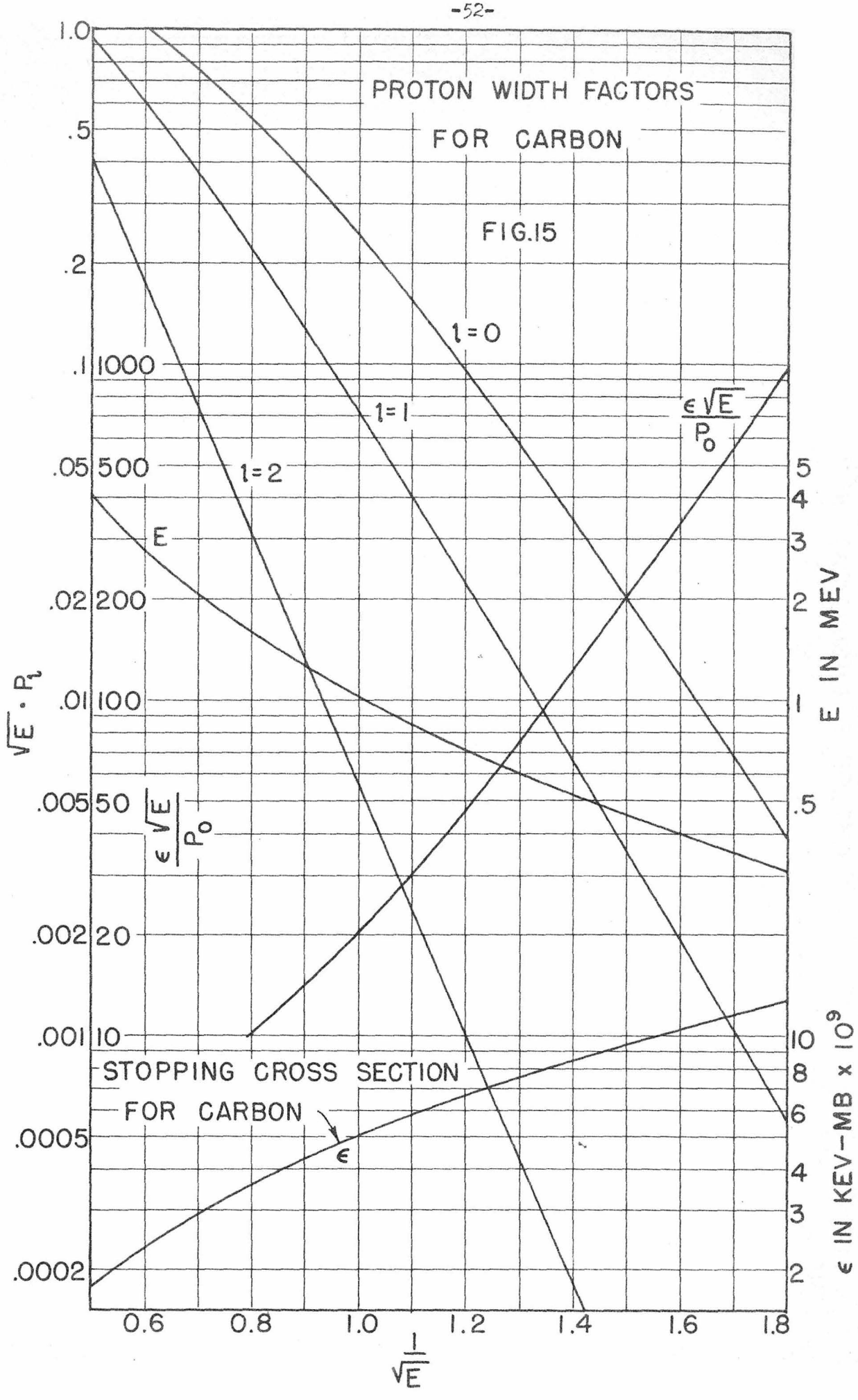
PROTON WIDTH FACTORS
FOR CARBON
FIG.15
l=0
l=1
l=2
E
$\frac{\epsilon\sqrt{E}}{P_0}$
$\sqrt{E}\cdot R_l$
E IN MEV
ε IN KEV-MB x 10^9
STOPPING CROSS SECTION
FOR CARBON
ε
1.0
.5
.2
.1
.05
.02
.01
.005
.002
.001
.0005
.0002
1000
500
200
100
50
20
10
5
4
3
2
1
.5
10
8
6
4
3
2
0.6
0.8
1.0
1.2
1.4
1.6
1.8
$\frac{1}{\sqrt{E}}$

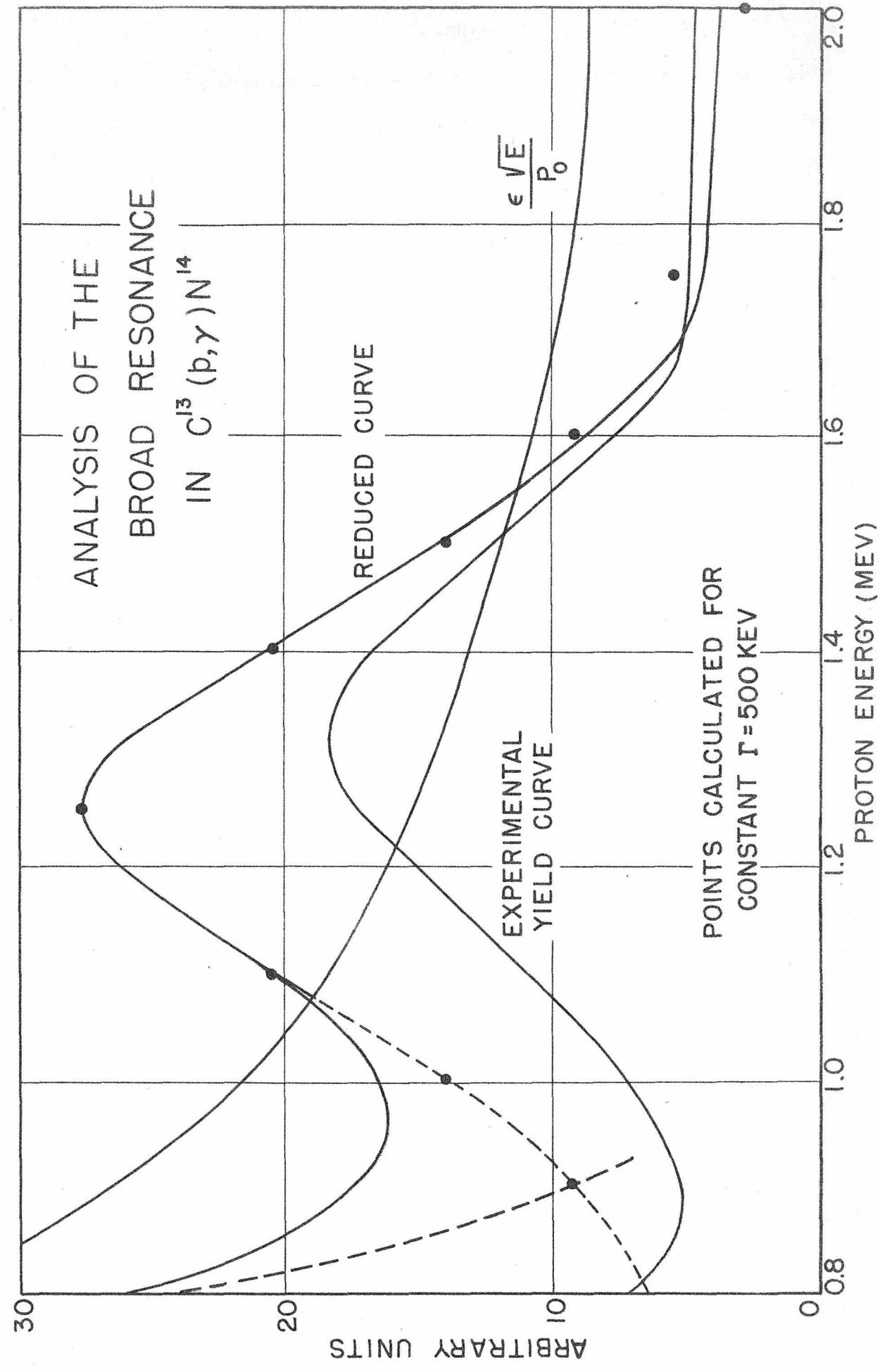
ANALYSIS OF THE
BROAD RESONANCE
IN $C^{13}(p,\gamma)N^{14}$
REDUCED CURVE
$\frac{\epsilon\sqrt{E}}{P_0}$
EXPERIMENTAL
YIELD CURVE
POINTS CALCULATED FOR
CONSTANT Γ=500 KEV
ARBITRARY UNITS
0
10
20
30
0.8
1.0
1.2
1.4
1.6
1.8
2.0
PROTON ENERGY (MEV)

FIG. 16

appearing in the resonance denominator is (still) not a constant, but has much less effect on the shape than do the multiplicative factors. The points plotted indicate how well the reduced curve may be fitted by a resonance term with (constant) $\Gamma = 500$ kev.

Although the penetration factors are known for each possible value of the angular momentum of the incoming protons, just which one is responsible for a particular resonance is not often known. An upper limit may be estimated by requiring that a state not decay faster than it can be formed, that is, in a time required to cross a nuclear diameter without collision. This corresponds to a width of a few Mev for 1 Mev protons. We may tabulate the reduced or nuclear widths for the several resonances.

TABLE V

Reaction	E_R (Mev)	Γ_p (kev)	G (kev)		
			$L = 0$	$L = 1$	$L = 2$
$C^{12}(p,\gamma)N^{13}$	.45	35	>1750	--	--
	1.70	70	117	230	1900
$C^{13}(p,\gamma)N^{14}$	.55	32.5	880	>4500	--
	1.16	6	18	60	670
	1.25	500	>1400	>4000	---
	1.76	2.1	3.2	7.2	42
	2.10	45	60	150	560

R. G. Thomas has shown[33] that this process may be in error for very broad resonances, so that the larger values (over 1 Mev) in the table should be somewhat larger. He uses a different parameter more intimately related to the nuclear wave functions.

It appears to be a secure conclusion that the 0.45 resonance with C^{12} and the 0.55 Mev and 1.25 Mev resonances with C^{13} are formed by capture of

s-wave ($L = 0$) protons. This conclusion is supported by the observation of isotropic radiation from the two low resonances reported by Devons and Hine[11].

From the absolute yields at the 0.55 and 1.76 Mev resonances, the relative yield of the thin target excitation function can be used with Equations (14), (24), and the absorption curves to give absolute values of $\omega\Gamma_\gamma$, and the resonance cross-sections can be found by Equation (13), of (26). The results of these calculations are summarized in Table VI:

TABLE VI

Reaction	E_R (Mev)	$Y_{max}(\infty)$* disint/proton	Γ_p (kev)	$\omega\Gamma_\gamma$ (ev)	σ_R (10^{-27} cm^2)
$C^{12}(p,\gamma)N^{13}$	0.45	7.6×10^{-10}	35	0.67	0.127
	1.70	1.1×10^{-9}	70	1.39	.035
$C^{13}(p,\gamma)N^{14}$	0.55	0.9×10^{-8}	32.5	8.6	1.44
	1.16	0.12×10^{-8}	6	1.3	0.56
	1.25	1.13×10^{-8}	500	12.8	0.062
	1.76	1.15×10^{-8}	2.1	14.8	12.0
	2.10	0.48×10^{-8}	45	6.15	1.96

* For thick targets of pure isotope. Values at 1.16 and 2.10 Mev calculated from $4\pi Y(90^\circ)$. All others are total yields.

XI. DISCUSSION

Without better information on the spectrum (of N^{14}) very few unequivocal conclusions can be drawn from the radiation widths found, even if the angular momentum of the radiating state (and hence ω) were known, since theoretical expressions for the widths contain nuclear "matrix elements", or quantum-mechanical averages involving the initial and final wave functions about which exact information is lacking. The expressions for radiation

widths referred to are, for

Electric 2^{ℓ} -pole: $$\Gamma_{\gamma} = \frac{4}{3}\left(\frac{r}{r_o}\right)^2 \times \left(\frac{\alpha E}{mc^2}\right)^{2\ell+1} mc^2, \text{ and for} \qquad (27a)$$

Magnetic Dipole: $$\Gamma_{\gamma} = \frac{1}{3}\alpha\left(\frac{\mu}{\mu_o}\right)^2\left(\frac{m}{M}\right)^2\left(\frac{E}{mc^2}\right)^3 mc^2 \text{ , where} \qquad (27b)$$

er^{ℓ} = matrix element for an electric 2^{ℓ}-pole transition,

r_o = e^2/mc^2, a convenient unit of length, about 0.8 x radius of N^{14}.

α = 1/(137), the fine-structure constant,

M/m = 1837, the ratio of proton to electron masses,

μ = the radiation magnetic moment, and

μ_o = the nuclear magneton.

137 mc^2 = 70 Mev, so even for $r = r_o$, electric quadrupole radiation of 7 Mev quanta will have a width 100 times smaller than for electric dipole. Magnetic dipole widths are of the same order as electric quadrupole. Since the nuclear wave functions are not known, we know only that r may be at most of the same order as the extent of the nucleus, say r_o, for the most favorable cases, and will frequently be considerably smaller.

Certain types of transitions are "forbidden", in that the matrix element can be expected to vanish if the differences in angular momenta and parity of the states in question do not have certain "allowed" values. These "selection rules" are for electric dipole:

$$\Delta J = 0, \pm 1, \quad \text{and parity changes;}$$

for electric quadrupole:

$$\Delta J = 0, \pm 1, \pm 2, \text{ and parity does not change;}$$

for magnetic dipole:

$$\Delta J = 0, \pm 1, \quad \text{and parity does not change.}$$

Another selection of which use will be made is that transitions between two states for <u>both</u> of which J = 0 are strictly forbidden.

These relations can be used in conjunction with all other information

available to choose the most consistent assignment of properties to the levels in question. We consider first the somewhat less complicated example of $C^{12}(p,\gamma)N^{13}$, which may be written out as

$$\begin{array}{ccccccc} C^{12} & (L\text{-wave}) & H^1 & \longrightarrow & (N^{13})^* & \longrightarrow & N^{13} \\ I = 0 & & s = 1/2 & & J & & I = 1/2 \\ \text{even} & & \text{even} & & & & \text{odd} \end{array} \quad + \quad \begin{array}{c} h\nu \\ (2^{\ell}\text{-pole}) \end{array} \tag{28}$$

The "spin" I = 0 for C^{12}, and it is taken to have even parity. The ground state of N^{13} is taken to have I = 1/2, and odd parity (in the shell model, this would be a proton loosely bound to a C^{12} core). For the 0.45 Mev resonance, which is surely formed by s-wave ($L = 0$) protons from its reduced width and isotropic radiation, the compound state at 2.4 Mev in N^{13} will have J = 1/2, and even parity. Then $\Delta J = 0$, with a change of parity for the transition to the ground state, and electric dipole radiation is allowed. The statistical factor is then unity, and $\Gamma_\gamma = 0.67$ ev. Inverting Equation (27a) for this width and 2.4 Mev radiation, we find $r = 0.154\ r_o$.

For the upper resonance, the situation is not so clear-cut. From Table V, (P. 54), the reduced width suggests only that $L \leq 2$ for the incoming proton. The state is at 3.5 Mev in N^{13}, and is observed to radiate directly to the ground state. The observed value of $\omega\Gamma_\gamma$ is 1.39 ev. $L = 1$ protons could form the excited state with J = 1/2 or 3/2 and odd parity, requiring electric quadrupole or magnetic dipole radiation. On that assumption, for J = 1/2: $r = 4.8\ r_o$ or $\mu = 3.4\ \mu_o$; while for J = 3/2: $r = 4.1\ r_o$ or $\mu = 2.4\ \mu_o$ -- in all cases insupportable results. For $L = 2$, J = 3/2 or 5/2, and the parity is even. Electric dipole radiation is again allowed, and we find for J = 3/2: $r = .09\ r_o$; while for J = 5/2: $r = .073\ r_o$. We cannot distinguish between J = 3/2 and 5/2 by this line of argument. Fortunately, Day[13] has studied the angular distribution of this radiation and finds it to have a term in $\cos^2\theta$ with a large negative coefficient (radiation strongest at 90°,

and symmetrical). Moreover, the coefficient varies with energy. Day finds the assignment of J = 3/2 and a small amount of interference from the lower resonance to best explain his results.

We may set up the same type of argument for $C^{13}(p,\gamma)N^{14}$, and write it

$$\begin{array}{ccccccc} C^{13} & + & H^1 & \rightarrow & (N^{14})^* & \rightarrow & N^{14} + h\nu \\ I = 1/2 \ (L - \text{wave}) & & s = 1/2 & & J & & I = 1 \quad (2^L - \text{pole}) \\ \text{odd} & & \text{even} & & & & \text{even} \end{array} \qquad (29)$$

Some question has arisen[30] about the assignment of even parity to the ground state of N^{14}, based on anomalies in the β-decay of O^{14} and C^{14} and the slow neutron $N^{14}(n,\gamma)N^{15}$ spectrum. Recent work by Butler, et. al[31] on the $N^{14}(d,p)N^{15}$ reaction with 7.9 Mev deuterons (stripping of a neutron from the deuteron) show that the ground state transition requires an angular momentum transfer $L_n = 1$, i.e., that the parities of N^{14} and N^{15} differ. We will consider the parity of N^{14} to be even.

For the 0.55 Mev resonance, which we assume formed by s-wave protons, the excited state can be formed with J = 0 or 1, and with odd parity. In either case, electric dipole radiation is allowed. If we assign the entire observed width to the ground state transition, then for J = 0: $\omega = 1/4$, $\Gamma_\gamma = 34$ ev., and $r = .177\ r_o$; for J = 1: $\omega = 3/4$, $\Gamma_\gamma = 11.5$ ev., and $r = .069\ r_o$, either of which is acceptable. If the branching ratio is 10% for a cascade process initiated by a 3 Mev γ, also by electric dipole radiation, then $r \simeq .2\ r_o$, in line with the above values. Assignment of J = 0 would forbid the 5.8 Mev direct transition to the first excited state at 2.3 Mev, which is almost surely J = 0 and even, as it is presumably the analogue of the C^{14} and O^{14} ground states (see below).

For the 1.76 Mev resonance, the nuclear width argument is useless. However, the anisotropic angular distribution observed by Day[13] excludes $L = 0$, and he finds the assignment J = 2, odd parity is consistent with his

results, although that assignment is not unique. In that case $\omega = 5/4$ and $\Gamma_\gamma = 11.8$ ev., which for electric dipole radiation gives $r = .0725\ r_o$.

For the 1.25 Mev resonance, we may again assume $L = 0$ protons, and obtain results very similar to the case of the 0.55 Mev resonance.

The evidence found in the scintillation measurements for a very soft component in this resonance only suggests the possibility of another mechanism at work in the decay of this particular case. We have remarked in the introduction that in these (p,γ) reactions the only competition is between radiation and re-emission of the proton. Any low states in N^{14} excited in a cascade process are "bound", and must radiate, since proton emission is no longer energetically possible. In the case of the 1.25 Mev resonance, it is separated from the 0.55 Mev resonance by only 650 kev (in the compound nucleus), and both have a nuclear width on the order of 1 Mev, so a transition between them might be much more probable than between two sharp levels. As the proton width for the lower resonance is several thousand times its radiation width, the suggested 0.65 Mev γ would not be followed by further radiation in this branch. To permit this soft radiation, it is necessary to assign different J values. If J = 0 for the 0.55 Mev resonance, J = 1 for the 1.25 Mev resonance. Why the upper state is forbidden to go to the 2.3 Mev level is left unanswered. A strictly ad hoc "explanation" might be found if the upper state were J = 1, but formed by $L = 1$ protons (reduced width > 4 Mev). It would then have even parity and be unable to go either to the ground state or the 2.3 Mev level by electric dipole radiation, in which case the observed branch would be decay by the favorable transition to the 8.05 Mev level. Were this actually the case, the broad resonance would not contribute to the yield at low energies, due to the even more rapid variation of the $L = 1$ barrier factor. Possibly an extension of Woodbury's technique to the region between 130 and 400 kev would clarify this point, as would the measurement of angular distributions.

For the 1.16 and 2.10 Mev resonances, it will be remarked only that the observed widths give values of $r \simeq 0.1\ r_o$ for 4 Mev electric dipole radiation.

Figure 17 is an energy level diagram for N^{14}, showing the levels now known, and the regions explored by this and other work. The reader is referred to Reference (1), P. 335 for a complete diagram, including the levels known above 11 Mev, with which we are not concerned here. It is clear that our cascades could take place in a number of ways. Only the very well established transitions have been indicated. The region of excitation between 9 1/2 and 10 1/2 Mev remains unexplored, and requires proton energies up to 3.2 Mev for the (p,γ) reaction. Also the region between 6.7 and 7.7 is inadequately explored. With the advent of thin C^{13} targets, the $C^{13}(d,n)N^{14}$ reaction may be used, and the yield of slow (threshold) neutrons investigated. 2.7 Mev deuterons would be necessary to reach the region covered by the (p,γ) reaction.

Also shown in Figure (17) are the levels of C^{14} and O^{14}. The ground states occur at the energies shown in parentheses, but when the Coulomb energy and $n^1 - H^1$ differences are removed, they correspond very well to the first excited state of N^{14}. Also shown is a level at 6.11 Mev in C^{14} found as a level in the residual nucleus in the $C^{13}(d,p)C^{14}$ reaction(32). This state must have $J \neq 0$ to radiate to the ground state ($I = 0$), and is presumably $J = 1$, odd parity, corresponding to electric dipole radiation(33). This state should correspond to an analogous level in N^{14} at 2.32 + 6.11 - .41 = 8.02 Mev, where 0.41 Mev is the anomalous level shift calculated from Thomas's theory*, By this analysis, the C^{14} level at 6.11 Mev is to be identified with the N^{14} level at 8.05 Mev. If this argument is correct, the 8.05 Mev

---

* R. G. Thomas, private communication.

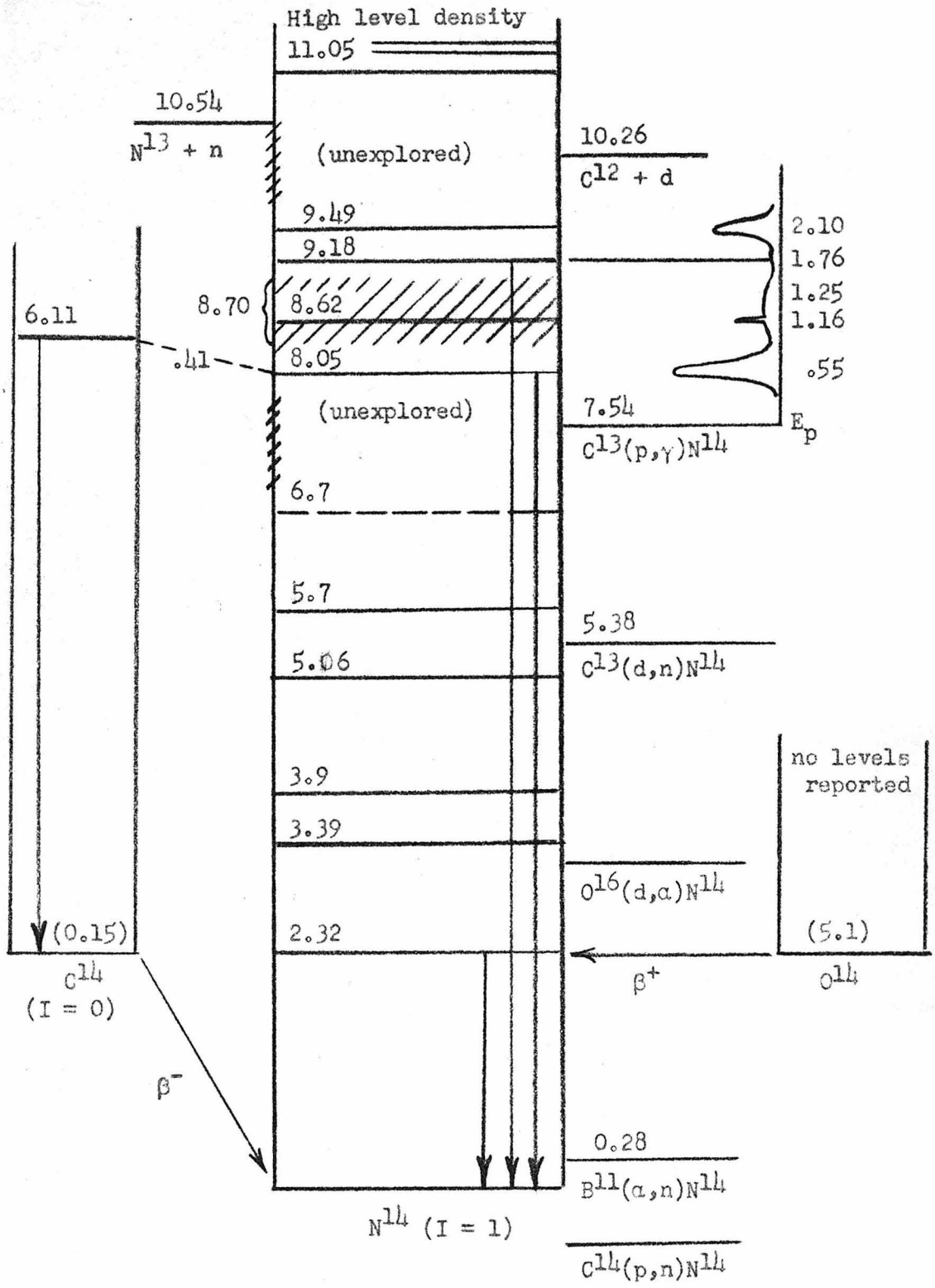
High level density
11.05
10.54
N^{13} + n
(unexplored)
10.26
C^{12} + d
9.49
9.18
2.10
1.76
1.25
1.16
.55
8.70
8.62
6.11
.41
8.05
(unexplored)
7.54
E_p
$C^{13}(p,\gamma)N^{14}$
6.7
5.7
5.38
5.06
$C^{13}(d,n)N^{14}$
no levels reported
3.9
3.39
$O^{16}(d,\alpha)N^{14}$
(0.15)
2.32
(5.1)
C^{14}
(I = 0)
β^+
O^{14}
β^-
0.28
$B^{11}(\alpha,n)N^{14}$
N^{14} (I = 1)
$C^{14}(p,n)N^{14}$

FIGURE 17

level must (also) have J = 1, odd parity and the 8.70 Mev level J = 0, odd parity, but a more complex explanation is required for the failure of the 8.05 Mev level to radiate to the 2.3 Mev level. This discrepancy is pointed to as another aspect of the anomalous behavior of N^{14} radiation.

The 2.32 Mev level has been assumed to have J = 0 and even parity as the analogue of the C^{14} and O^{14} ground states, but this assignment, on which some of the above discussion depends, is not altogether secure, as the $O^{14}(\beta^+)N^{14}$ decay is observed to go primarily to this excited state (apparently a 0-0 transition, highly forbidden by Gamow-Teller rules, not by Fermi rules), with a large transition probability, while the $C^{14}(\beta^-)N^{14}$ goes to the ground state ($\Delta J = 1$) with an anomalously <u>low</u> transition probability.

The measured magnetic moment of the ground state of N^{14} implies a strong mixture of "spectroscopic" states, or looked at in another way, that the L - S coupling model is inadequate to give a unique description. If this is the case, it may not be surprising to find strong branching and other anomalies in the radiation from the excited states. N^{14} has seven neutrons and seven protons, and is the heaviest of the four known stable "odd-odd" (!) nuclei. The next lightest, B^{10}, was found to have I = 3 and likewise to emit rather complex radiation.

CONCLUSION

Five states in N^{14} have been investigated, and shown to emit a complex radiation spectrum, suggesting and challenging further experimental and theoretical work. The next important step should be an all-out attack on the energies, intensities, and branching ratios of the spectrum. It is hoped that the new techniques of scintillation spectroscopy may prove a useful tool in that investigation. The properties of more levels in regions of excitation not yet investigated may supply additional information.

The final dénouement of the character of N^{14} should have important implications in the general theory of nuclear states.

REFERENCES

1. Hornyak, Lauritsen, Morrison, and Fowler, Rev. Mod. Phys. 22, 291 (1950).
2. Roberts and Heydenburg, Phys. Rev. 53, 374 (1938).
3. Curran, Dee, and Petrzilka, Proc. Roy. Soc. 169, 269 (1939).
4. Hole, Holtzmark, and Tangen, Zeits. f. Physik 118, 48 (1941).
5. Fowler and Lauritsen, Phys. Rev. 76, 314 (1949).
6. R. Tangen, Kgl. Nord. Vid. Selsk. Scr. No. 1 (1946).
7. D. M. Van Patter, Phys. Rev. 76, 1264 (1949).
8. Woodbury, Hall, and Fowler, Phys. Rev. 75, 1462 (1949).
9. Hall and Fowler, Phys. Rev. 77, 197 (1950).
10. Bailey and Stratton, Phys. Rev. 77, 194 (1950).
11. Devons and Hine, Proc. Roy. Soc. 199, 56 and 73 (1949).
12. Goldhaber, Williamson, Jackson, and Laubenstein (private communication).
13. R. B. Day, PhD Thesis, California Institute of Technology (1951). See also
13a. R. B. Day and J. Perry, Jr. Phys. Rev. 81, 662A (1951).
14. D. B. Duncan, Phys. Rev. 76, 587A (1949).
15. Ashby and Hanson, Rev. Sci. Inst. 13, 128 (1942).
16. J. E. Perry, Jr., et. al., Rev. Sci. Inst. (In Press).
17. G. C. Phillips, Phys. Rev. 80, 164 (1950).
18. J. E. Richardson, PhD Thesis, The Rice Institute (1950). See also
18a. Phillips and Richardson, Rev. Sci. Inst. 21, 885 (1950).
19. Fowler, Lauritsen, and Lauritsen, Rev. Mod. Phys. 20, 236 (1948).
20. Bernet, Herb, and Parkinson, Phys. Rev. 54, 398 (1938).
21. Grove, Copper, and Harris, Phys. Rev. 80, 107 (1950).
22. Li and Whaling, Phys. Rev. 82, 122 (1951).
23. A. W. Schardt, PhD Thesis, California Institute of Technology (1951).
24. Walker and Day, Bull. Am. Phys. Soc., D-10, April 26 (1951).
25. Chao, Tollestrup, Fowler, and Lauritsen, Phys. Rev. 79, 108 (1950).

26. Hornyak and Lauritsen, Phys. Rev. 77, 160 (1950).

27. Breit and Wigner, Phys. Rev. 49, 519 (1936).

28. Christy and Latter, Rev. Mod. Phys. 20, 185 (1948).

29. E. J. Woodbury, PhD Thesis, California Institute of Technology (1951).

30. E. Gerjuoy, Phys. Rev. 81, 62 (1951).

31. S. T. Butler, Phys. Rev. 80, 1095 (1950).

32. Thomas and Lauritsen, Phys. Rev. 78, 88 (1950).

33. R. G. Thomas, PhD Thesis, California Institute of Technology (1951).